AMERICAN SOCIETY FOR MICROBIOLOGY | Applied and Environmental Microbiology®

ENVIRONMENTAL MICROBIOLOGY

Novel Cholera Toxin Variant and ToxT Regulon in Environmental *Vibrio mimicus* Isolates: Potential Resources for the Evolution of *Vibrio cholerae* Hybrid Strains

Sucharit Basu Neogi,[a] Nityananda Chowdhury,[a]* Sharda Prasad Awasthi,[a] Masahiro Asakura,[a] Kentaro Okuno,[a] Zahid Hayat Mahmud,[b] Mohammad Sirajul Islam,[b] Atsushi Hinenoya,[a] Gopinath Balakrish Nair,[c] Shinji Yamasaki[a]

[a]Graduate School of Life and Environmental Sciences, Osaka Prefecture University, Izumisano, Osaka, Japan
[b]International Centre for Diarrhoeal Disease Research, Bangladesh, Dhaka, Bangladesh
[c]Translational Health Science and Technology Institute, Gurgaon, Haryana, India

ABSTRACT Atypical El Tor strains of *Vibrio cholerae* O1 harboring variant *ctxB* genes of cholera toxin (CT) have gradually become a major cause of recent cholera epidemics. *Vibrio mimicus* occasionally produces CT, encoded by *ctxAB* on CTXΦ genome; toxin-coregulated pilus (TCP), a major intestinal colonization factor; and also the CTXΦ-specific receptor. This study carried out extensive molecular characterization of CTXΦ and ToxT regulon in *V. mimicus ctx*-positive (*ctx*$^+$) strains (i.e., *V. mimicus* strains containing *ctx*) isolated from the Bengal coast. Southern hybridization, PCR, and DNA sequencing of virulence-related genes revealed the presence of an El Tor type CTX prophage (CTX^{ET}) carrying a novel *ctxAB*, tandem copies of environmental type pre-CTX prophage (pre-CTX^{Env}), and RS1 elements, which were organized as an RS1-CTX^{ET}-RS1-pre-CTX^{Env}-pre-CTX^{Env} array. Additionally, novel variants of *tcpA* and *toxT*, respectively, showing phylogenetic lineage to a clade of *V. cholerae* non-O1 and to a clade of *V. cholerae* non-O139, were identified. The *V. mimicus* strains lacked the RTX (repeat in toxin) and TLC (toxin-linked cryptic) elements and lacked *Vibrio* seventh-pandemic islands of the El Tor strains but contained five heptamer (TTTTGAT) repeats in *ctxAB* promoter region similar to those seen with some classical strains of *V. cholerae* O1. Pulsed-field gel electrophoresis (PFGE) analysis showed that all the *ctx*$^+$ *V. mimicus* strains were clonally related. However, their *in vitro* CT production and *in vivo* toxigenicity characteristics were variable, which could be explainable by differential transcription of virulence genes along with the ToxR regulon. Taken together, our findings strongly suggest that environmental *V. mimicus* strains act as a potential reservoir of atypical virulence factors, including variant CT and ToxT regulons, and may contribute to the evolution of *V. cholerae* hybrid strains.

IMPORTANCE Natural diversification of CTXΦ and *ctxAB* genes certainly influences disease severity and shifting patterns in major etiological agents of cholera, e.g., the overwhelming emergence of hybrid El Tor variants, replacing the prototype El Tor strains of *V. cholerae*. This report, showing the occurrence of CTX^{ET} comprising a novel variant of *ctxAB* in *V. mimicus*, points out a previously unnoticed evolutionary event that is independent of the evolutionary event associated with the El Tor strains of *V. cholerae*. Identification and cluster analysis of the newly discovered alleles of *tcpA* and *toxT* suggest their horizontal transfer from an uncommon clone of *V. cholerae*. The genomic contents of ToxT regulon and of tandemly arranged multiple pre-CTXΦ^{Env} and of a CTXΦ^{ET} in *V. mimicus* probably act as salient raw materials that induce natural recombination among the hallmark virulence genes of hybrid *V. cholerae* strains. This report provides valuable information to enrich our knowledge on the evolution of new variant CT and ToxT regulons.

Citation Neogi SB, Chowdhury N, Awasthi SP, Asakura M, Okuno K, Mahmud ZH, Islam MS, Hinenoya A, Nair GB, Yamasaki S. 2019. Novel cholera toxin variant and ToxT regulon in environmental *Vibrio mimicus* isolates: potential resources for the evolution of *Vibrio cholerae* hybrid strains. Appl Environ Microbiol 85:e01977-18. https://doi.org/10.1128/AEM.01977-18.

Editor Eric V. Stabb, University of Georgia

Address correspondence to Shinji Yamasaki, shinji@vet.osakafu-u.ac.jp.

* Present address: Nityananda Chowdhury, Medical University of South Carolina, Charleston, South Carolina, USA.

S.B.N. and N.C. contributed equally to this article.

Received 16 August 2018
Accepted 29 October 2018
Accepted manuscript posted online 16 November 2018
Published 23 January 2019

KEYWORDS CTXΦ, El Tor biotype, *Vibrio cholerae*, *Vibrio mimicus*, cholera toxin, classical biotype, *tcpA*, *toxT*

Vibrio mimicus is genetically and ecologically very similar to *Vibrio cholerae*, the cholera bacterium, and shares similar environmental niches in freshwater and estuarine ecosystems, particularly in tropical regions such as the Bengal delta. *V. mimicus* is known to be associated with sporadic cholera-like diarrhea cases. Despite extensive efforts at hygiene promotion and therapeutic advances, cholera continues to pose as a major health problem worldwide, accounting for millions of episodes and thousands of deaths, with ca. 132,000 cases in 2016 reported to the World Health Organization (http://www.who.int/gho/epidemic_diseases/cholera/en/). The principal pathogenic factor instigating the disease is the cholera toxin (CT), encoded by the *ctxAB* operon, predominantly found in *V. cholerae* strains belonging to the O1 and O139 serogroups and occasionally in a few non-O1/non-O139 serogroups. Among the seven known cholera pandemics, the El Tor biotype of *V. cholerae* O1 is associated with the current, seventh pandemic since 1961 whereas the counterpart classical biotype was associated with the sixth pandemic. In Bangladesh, the classical form of cholera reemerged in 1983, was later detected at diminishing levels as a consequence of the rise in El Tor cholera, and is believed to have been extinct since 1993 (1). However, since the last decade, hybrid El Tor strains producing classical CT have been the dominant cause of epidemic and endemic cholera, replacing the prototype El Tor strains that produce El Tor CT (1). Occurrences of such variant El Tor strain types have also been reported to have spread in many countries in Asia and Africa and in Haiti (2–4). This indicates a cryptic existence of the variant or classical *ctxB* gene and variant CTXΦ in environmental reservoirs that has so far been left mostly unexplored. *In vitro* experiments have shown that CTXΦ can infect certain *V. mimicus* strains (5). In line with this, although rarely isolated, the occurrence of the *ctxAB* gene among *V. mimicus* strains in Bangladesh, India, Japan, and the United States attests to the hypothesis of interspecies genetic exchange (6–9).

The *ctx*AB operon encoding the A and B subunits of CT is a part of the genome of CTXΦ, a filamentous bacteriophage. The precursor form of the CTXΦ, pre-CTXΦ, does not carry the *ctxAB* genes (10). Before this study, a total of 13 genotypes of *ctxB* have been distinguished based on single nucleotide polymorphisms (SNPs) at 10 loci of this toxigenic factor (see Table 2). Notably, *ctxB* genotypes 1 and 2 are typical of all classical strains and El Tor strains from Australia, respectively, while genotypes 3 and 7 are featured among the pandemic El Tor and the Haitian variant strains. *V. cholerae* O1 El Tor strains are also characterized by the presence of TLC (toxin-linked cryptic) element and RTX (repeat in toxin) genes in the flanking region of CTX prophage and of two large genomic islands termed *Vibrio* seventh pandemic island I (VSP-I) and VSP-II (11). Other known virulence factors of *V. cholerae*, particularly of the non-O1/non-O139 strains, include heat-stable enterotoxin/NAG-ST (encoded by *stn*), the type III secretion system (TTSS) (*vcsN2*), and cytotoxic cholix toxin (*chxA*) (12, 13). Natural recombination events, compounded with the integration of phages, contribute to the evolution of genes, especially those related to virulence and ecological fitness (14). While persisting in the aquatic environment, *V. cholerae* and *V. mimicus* interact with diverse phages, and a portion of their populations, harboring a selective receptor, can integrate toxigenic phages into their genome (6).

The CTXΦ genome (~6.9 kb) contains core and RS2 regions. The core region includes genes involved in phage morphogenesis and CT production, including *ctxAB*, *zot*, and *orfU* (or "gIII$^{CTX\Phi}$"). The RS2 region contains genes required for replication (*rstA*), integration (*rstB*), and regulation (*rstR*) of CTXΦ (15). Moreover, the upstream promoter of *ctxAB* possesses heptamer repeats, considered an evolutionary signature, while its downstream intergenic region (ig) contains a site for CTXΦ integration, mediated by XerC and XerD recombinases (16). In El Tor strains, the prophage DNA is flanked by a genetic element known as RS1, which is a satellite phage (17). In comparison to RS2, the

RS1 additionally contains *rstC*, which encodes an antirepressor of *rstR* and promotes transmission of RS1 and CTXΦ (18). In *V. cholerae* strains, the presence of both CTX prophage and the RS1 element, in the form of solitary and multiple copies with diverse arrays of genetic organization, has been documented (19, 20). On the basis of nucleotide sequence polymorphism in its several genes, including *rstR* and *orfU*, the CTX prophage can be differentiated into several types such as the classical, El Tor, Kolkata, and environmental types (20). Among the El Tor variant or hybrid strains, different *ctxB* genotypes, including classical *ctxB1* and Haitian *ctxB7* and occurring predominantly in classical and El Tor types of CTX prophages, have been reported (2, 3, 19, 21). Although extensive investigations have revealed nucleotide sequence polymorphism and diversity in the array of CTX prophages in the *V. cholerae* genome (19–22), little is known of those *V. mimicus* strains.

The transmission of CTXΦ into a *Vibrio* strain relies on the presence of a specific cell surface type IV pilus receptor, termed the toxin-coregulated pilus (TCP), which also plays a vital role, aiding colonization of *V. cholerae* in human or animal intestine (23). The TCP is located on the *Vibrio* pathogenicity island (VPI) and is produced by the action of a cluster of genes, termed the TCP island. The major structural subunit of TCP is encoded by *tcpA* (14). The expression of CT and TCP is activated by ToxT, present on the TCP island, and is under the control of the ToxR regulon, comprising *toxR*, *toxS*, *tcpP*, and *tcpH* (24). On the basis of the nucleotide sequence polymorphism in *tcpA*, the TCP can be differentiated into several types, e.g., El Tor, classical, Nandi, and Novais (25). CTX/pre-CTX prophages and genes of VPIs are found scattered throughout environmental isolates of *V. cholerae* (22). Despite the absence of the classical biotype strains along with the classical CTX phage (1), the increasing occurrence of hybrid El Tor strains of *V. cholerae* O1 harboring variant *ctxB* genes is intriguing and requires detailed exploration for determination of their environmental reservoirs. Being genetically and ecologically the two most closely related species, there is a high probability of genetic exchange between *V. mimicus* and *V. cholerae*, particularly among their populations interacting closely in the environment. Therefore, some *V. mimicus* strains may act as a potential reservoir of virulence genes associated with cholera and diarrhea epidemics. However, our knowledge of the traits and diversity of genetic determinants of virulence, particularly that associated with cholera-like diarrhea, in *V. mimicus*, and their similarity to those of epidemic strains of *V. cholerae* is very limited. In this study, several *V. mimicus ctx*-positive (*ctx*$^+$) strains (i.e., *V. mimicus* strains containing *ctx*) isolated from estuarine surface waters in Bangladesh were analyzed to ascertain whether they can act as reservoirs of the CTXΦ-carrying *ctxAB* variant present in *V. cholerae* strains associated with recent epidemics. The objectives were to investigate (i) the molecular diversity of genetic elements within CTX prophage and TCP islands, (ii) *in vitro* CT production, (iii) *in vivo* fluid accumulation using a suckling mouse model, and (iv) differential expression of the ToxT regulon in these environmental *V. mimicus* strains. Comparison of these phenotypic and genetic traits to those of toxigenic *V. cholerae* would aid in improving understanding the evolution of new variant CT and ToxT regulon.

RESULTS

Antimicrobial susceptibility. With regard to the increasing threat of multidrug resistance, *V. mimicus* strains were tested for antimicrobial susceptibility, which also partly demonstrated their phenotypic variations. Among the 11 antimicrobials tested, polymyxin B is also known as a phenotypic signature of the El Tor and corresponding hybrid strains of *V. cholerae* (1). All *ctx*$^+$ *V. mimicus* strains showed resistance to ampicillin (10 μg) and cephalothin (30 μg) and intermediate resistance to erythromycin (15 μg). However, two types of antimicrobial resistance pattern were observed based on the resistance to polymyxin B (50 μg) and gentamicin (10 μg) (Table 1). Three of six *V. mimicus* strains showed resistance to polymyxin B (50 μg), while the other three strains showed intermediate resistance to gentamicin (10 μg).

PFGE-based screening for genomic relatedness. Pulsed-field gel electrophoresis (PFGE) of the undigested genomic DNA (gDNA) showed that the *ctx*$^+$ *V. mimicus* strains

TABLE 1 Antimicrobial susceptibility, cholera toxin production, PFGE patterns, and enterotoxigenicity in *ctx*$^+$ *V. mimicus* strains

Strain ID[a]	Date of isolation	Antimicrobial resistance (μg)[b]						PFGE pattern		CT production[d] (ng ml^{-1})		Suckling mouse assay[e] (n = 5)	
		PB (50)	CF (30)	EM (15)	ABPC (10)	GM (10)	Others[c]	SfiI	NotI	LB	AKI	FA ratio	Diarrhea
V. mimicus DCT1	17 July 2000	R	R	I	R	S	S	I	a	0.3	0.1	nd	nd
***V. mimicus* DCT2**	**05 August 2000**	**R**	**R**	**I**	**R**	**S**	**S**	**II**	**a**	**0.4**	**0.2**	**0.068**	**0/5**
V. mimicus DCT3	22 August 2000	R	R	I	R	S	S	I	b	0.2	0.1	nd	nd
V. mimicus DCT4	11 September 2000	S	R	I	R	I	S	III	b	0.2	0.1	nd	nd
***V. mimicus* DCT5**	**03 October 2000**	**S**	**R**	**I**	**R**	**I**	**S**	**II**	**b**	**110**	**30**	**0.087**	**5/5**
V. mimicus DCT6	27 October 2000	S	R	I	R	I	S	II	a	0.5	0.4	nd	nd
V. cholerae 0395	1948	S	I	S	R	S				270	150	0.098	5/5
V. cholerae N16961	1975	R	S	S	I	S				1.6	2.5	nd	nd

[a]"DCT1" to "DCT6" represent *V. mimicus* strains examined in this study; "O395" and "N16961" represent *V. cholerae* reference strains of classical and El Tor biotypes, respectively. ID, identifier. Boldface highlighting indicates data from low-CT-producing *V. mimicus* strain DCT2 and from high-CT-producing *V. mimicus* strain DCT5.
[b]"PB," "CF," "EM," "ABPC," and "GM" indicate polymyxin B, cephalothin, erythromycin, ampicillin, and gentamicin, respectively. S, R, and I designate susceptible, resistant, and intermediate patterns, respectively.
[c]Others, other antibiotics (e.g., furazolidone, trimethoprim-sulfamethoxazole, nalidixic acid, ciprofloxacin, and tetracycline) were also used at standard doses (i.e., 100, 1.25/23.75, 10, 5, and 30 μg, respectively).
[d]CT production was measured by bead-ELISA after cells were cultured (4 h static plus 4 h shaking, 120 revolutions min^{-1}) in Luria-Bertani broth and AKI medium, representing inducible conditions for the classical and El Tor strain types, respectively. Mean values given are based on three experiments performed for each strain.
[e]A fluid accumulation (FA) ratio of >0.08 in the suckling mouse assay indicates enterotoxigenicity. Mean values (n = 5) are given. nd, not done.

possessed ca. 2.9 and 1.3 Mb of large and small chromosomes, respectively, which were similar to sizes seen with the *V. mimicus* type strain (ATCC33539^T). Interestingly, the small chromosome in *V. mimicus* strains was larger (ca. 0.2 Mb) than those in the classical (O395), El Tor (N16961), and non-O1/non-O139 strains of *V. cholerae* E233 (VCE233) (Fig. 1). PFGE analysis of NotI- and SfiI-digested gDNA of *ctx*$^+$ *V. mimicus* strains showed 1-to-2-band differences that resulted in two (a and b) and three (I, II, and III) subtypes, respectively (Fig. 1 and Table 1). According to criteria previously specified by Tenover et al. (26), these strains are clonal, since they did not differ by more than 6 bands. However, combining the NotI and SfiI patterns resulted in categorization of these six strains into four subtypes (Ia, Ib, IIb, and IIIb).

Occurrence of the major virulence factors. Among the hallmark genes associated with the toxigenic *V. cholerae* strains, several related to CT production were detected in the *V. mimicus* strains used in this study. Colony blot hybridization showed the presence of *ctxA* and *zot* of CTXΦ, *rstC* of the RS1 element, and *tcpA* of the VPI. However, these strains did not harbor genes representing VSP-I and VSP-II. They were also negative for TLC and RTX elements, which are commonly present in the flanking region of CTXΦ in *V. cholerae* El Tor and corresponding hybrid strains. No other important virulence genes of *V. cholerae*, namely, *vcsN2*, *chxA*, and *stn*, encoding type III secretion system (ATPase), cholix toxin, and heat-stable enterotoxin (NAG-ST), respectively, were detected in the *ctx*$^+$ *V. mimicus* strains.

Characteristics of *ctxAB*, *orfU*, and CTXΦ-associated genetic elements. On the basis of the results of the mismatch amplification mutation assay (MAMA)-PCR, all the *V. mimicus* strains contained the classical type of the *ctxB* gene. Sequencing of the entire *ctxB* gene revealed that all instances of the gene were identical in all six *V. mimicus* strains. Although showing signature changes at positions 39 (tyrosine to histidine) and 68 (isoleucine to threonine), similarly to classical *ctxB* genotype 1, the *V. mimicus ctxB* gene had additional nonsynonymous substitutions conferring subtle changes in the deduced amino acids at positions 46 (phenylalanine/F to leucine/L) and 67 (alanine/A to glutamic acid/E) (Table 2). Comparative analyses performed with other known *ctxAB* genotypes reported among *V. mimicus* and *V. cholerae* strains revealed the existence of a new *ctxB* gene, which was designated genotype 14. This genotype was almost identical to genotype 12, reported from a *V. mimicus* strain which also contains leucine at position 46 but contains alanine at position 67 (Table 2) (Fig. 2). Notably, in all other genotypes of *ctxB* identified so far, alanine is present at position 67 (Table 2).

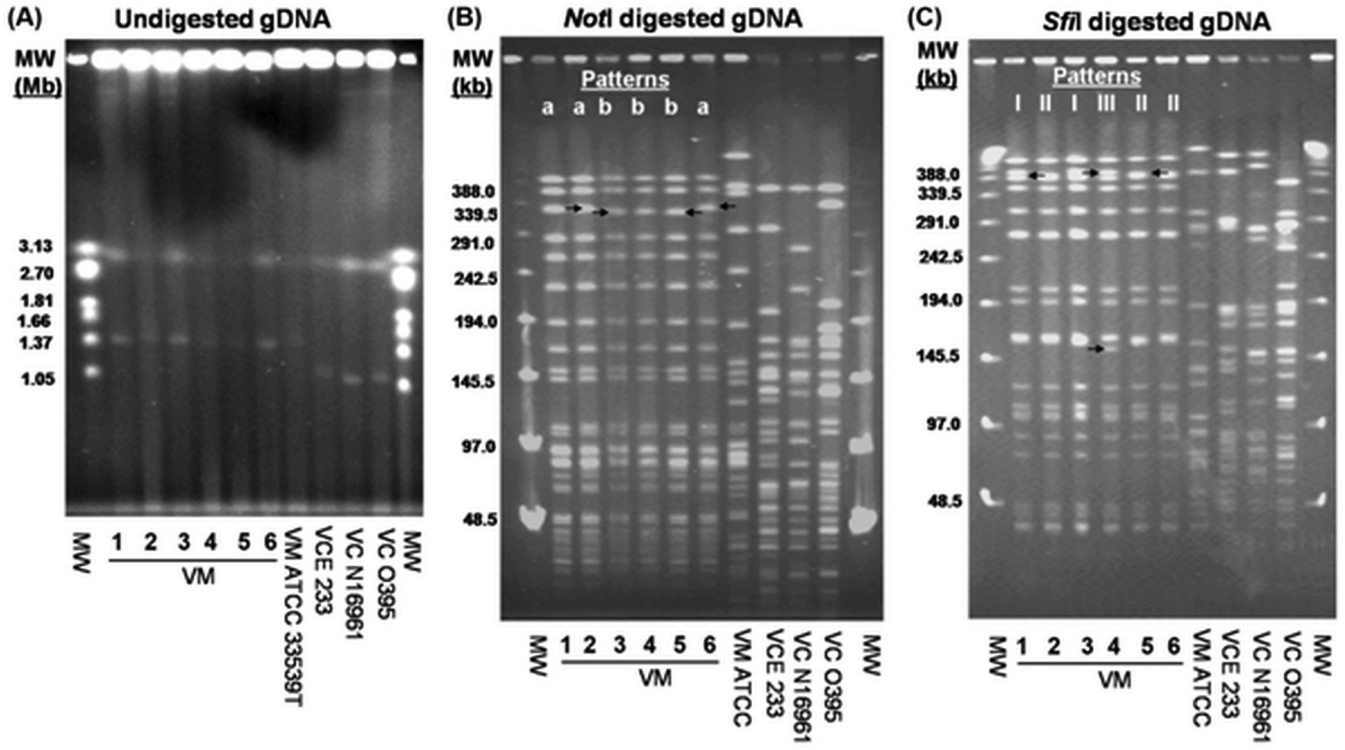

FIG 1 PFGE analysis of environmental *ctx*$^+$ and reference (ATCC) strains of *V. mimicus* (VM) and of *ctx*$^+$ non-O1/non-O139 (VCE 233), O1 El Tor (VC N16961), and O1 classical (VC O395) strains of *V. cholerae*. (A) Gel image of PFGE profiles of undigested gDNA showing similar sizes of the two chromosomes of *ctx*$^+$ *V. mimicus* and ATCC *V. mimicus* strains. (B and C) Gel images showing PFGE patterns of NotI-digested (B) and SfiI-digested (C) gDNA of *ctx*$^+$ *V. mimicus* and the reference strains. The *ctx*$^+$ *V. mimicus* strains were clonal but differed in 1 to 2 bands, indicated by arrows. NotI- and SfiI-digested gDNA of *ctx*$^+$ *V. mimicus* strains generated two (a and b) and three (I, II, and III) PFGE profiles, respectively. "MW" represents the molecular weight standard of the *Hansenula wingei* chromosomes (Bio-Rad) for undigested gDNA (A) and lambda ladder (Bio-Rad) for digested gDNA (B and C).

Sequencing analysis of *ctxA* of *V. mimicus* strains also showed alterations from the canonical *ctxA* sequences. This novel *ctxA* sequence differed from that of the reference El Tor and classical strains at three amino acid positions, namely, positions 46, 190, and 198, while the highest similarity was observed with *ctxA* of a *V. mimicus* strain with *ctxB*

TABLE 2 Comparative diversity levels in the *ctxAB* gene among *V. mimicus* and *V. cholerae* strains

Strain (GenBank accession no.)[a]	Isolation		*ctxA* (aa position)[b]					*ctxB* (aa position)[c]										Designated genotype	Reference
	Country(ies)	Yr(s)	46	190	198	226	255	20	24	28	34	36	39	46	55	67	68		
V. cholerae O1, CL, O395 (CP000627)	India	1948	S	R	I	V	K	H	Q	D	H	T	**H**	F	K	A	**T**	1	1
V. cholerae O1, ET, Australia	Australia							H	Q	D	H	T	**H**	L	K	A	**T**	2	1
V. cholerae O1, ET, N16961 (NC_002505)	Bangladesh	1975	S	R	I	V	K	H	Q	D	H	T	**Y**	F	K	A	**I**	3	1
V. cholerae O139 (FJ821557)	Bangladesh	1998						H	Q	D	H	T	**Y**	F	K	A	**T**	4	1
V. cholerae O139 (FJ821556)	Bangladesh	2005						H	Q	A	H	T	**H**	F	K	A	**T**	5	1
V. cholerae O139 (FJ821581)	Bangladesh	2007						H	Q	D	P	T	**Y**	F	K	A	**T**	6	1
V. cholerae O1 (EU496273, NC_016445)	India, Haiti	2007, 2010						N	Q	D	H	T	**H**	F	K	A	**T**	7	1
V. cholerae O27 (AF390572)	Japan	1996	S	R	I	V	E	H	H	A	H	T	**H**	F	K	A	**T**	8	1
V. cholerae O37 (D30052)	Sudan	1968	N	R	I	V	K	H	Q	D	H	T	**H**	L	N	A	**T**	9	1
V. cholerae O1 (EU932878)	Zambia	1996						H	Q	D	P	T	**Y**	F	K	A	**I**	10	54
V. cholerae O1 (EU932881)	Zambia	2003						H	Q	D	P	T	**H**	F	K	A	**T**	11	54
V. mimicus (ACYV01000039)	USA	1990	N	I	I	I	K	H	Q	D	H	T	**H**	L	K	A	**T**	12	55
V. cholerae O1 (KC754370)	China	1965						H	Q	D	H	A	**Y**	L	N	A	**T**	13	56
V. mimicus (LC427969)	Bangladesh	2000	N	I	**V**[d]	V	K	H	Q	D	H	T	**H**	L	K	**E**[d]	**T**	14	This study

[a]Known serogroups of *V. cholerae* strains are shown. Accession numbers of the gene sequences are given in parentheses.

[b]The deduced amino acid (aa) positions are indicated by the given numbers; only the variable amino acids deduced from *ctxA* gene sequences available from 7 of 14 representative strains of *V. cholerae* and *V. mimicus* are shown.

[c]The deduced amino acid (aa) positions are indicated by the given numbers; only the variable amino acids deduced from the *ctxB* gene among the representative strains of *V. cholerae* and *V. mimicus* are shown. Boldface data for positions 39 and 68 indicate the amino acid markers, differentiating classical and El Tor type *ctxB* genes.

[d]Unique change in deduced amino acid of *ctxAB* in *V. mimicus* strains of this study.

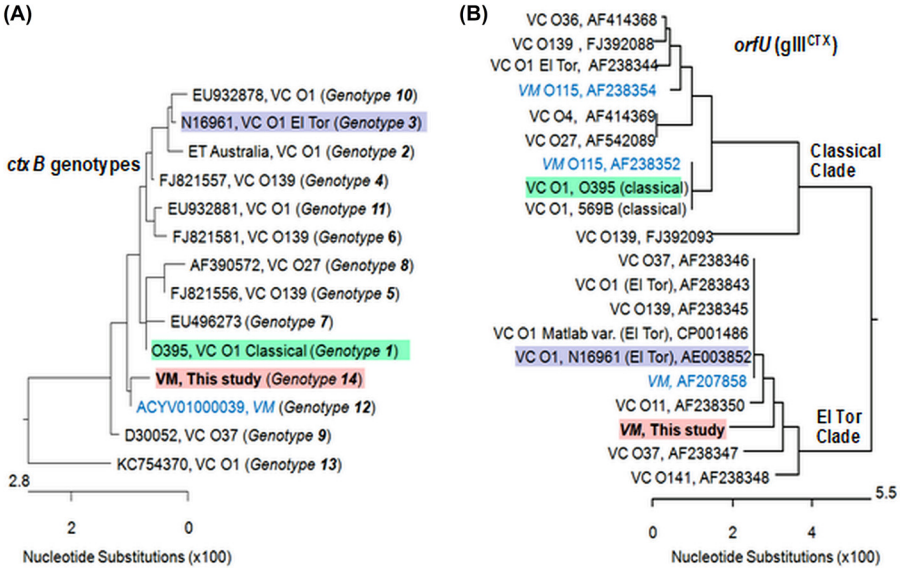

FIG 2 Genetic relatedness among *ctxB* and *orfU* genes of *V. mimicus* and *V. cholerae* strains. (A) Novel *ctxB* genotype 14 of *V. mimicus* showed the highest affiliation with genotype 12, reported to occur in a *V. mimicus* strain isolated from the United States. However, *ctxB* genotype 14 showed more closeness with both *ctxB* genotype 1 and *ctxB* genotype 7, representing classical and Haitian strains, respectively, in comparison to genotype 3, usually found in the typical El Tor strains of *V. cholerae* O1. (B) The *orfU* gene of *V. mimicus* of this study showed close affiliation to the strains grouped into the El Tor clade of *V. cholerae*.

genotype 12 (Table 2). A unique change from isoleucine to valine at position 198 of *ctxA* in the *V. mimicus* strains was noteworthy.

Because the *orfU* gene is important in studying the diversity in the core region of CTX prophage, this gene was also sequenced and phylogenetic analysis was done. Interestingly, complete sequence homology among all the *V. mimicus* strains and also within CTXΦ^{ET} and pre-CTXΦ^{Env} prophages was observed. Comparative analyses of OrfU (pIII^{CTX}) sequences performed with the reference El Tor strain and classical strains of *V. cholerae* and a recently studied *V. mimicus* strain indicated that the *V. mimicus* strains of this study did not have 100% sequence similarity with any of them but rather they possessed nine unique changes with a total of 31 polymorphic sites. The data showed a high level of similarity of *V. mimicus* OrfU to that of *V. cholerae* El Tor strain N16961, with 11 polymorphic sites, whereas with *V. cholerae* classical strain O395 and the other *V. mimicus* strain, there were 27 amino acid substitutions (see Fig. S1 in the supplemental material). Thus, sequencing analysis indicated that these *V. mimicus* strains carried a variant OrfU in their CTXΦ genome. In phylogenetic analysis, the *orfU* sequences of these *V. mimicus* strains did not cluster with partial (702 of 1,083 nucleotides) *orfU* sequences of classical *V. cholerae* available in GenBank database; instead, they grouped with El Tor, El Tor variant, and O139 strains and with several non-O1/non-O139 strains of *V. cholerae* (Fig. 2).

The presence of RS1 element was confirmed by *rstC* gene-based PCR (Fig. S1), followed by sequencing analysis. The *rstC* gene in the *V. mimicus* strains was identical to that in the reference El Tor strain. PCR-based genotyping of *rstR* showed the presence of two different alleles, the El Tor type (*rstR*^{ET}) and the environmental type (*rstR*^{Env}), indicating the occurrence of multiple prophages, i.e., CTXΦ^{ET} and CTXΦ^{Env}.

Genetic organization of CTXΦ-associated elements. Southern hybridization of chromosomal DNA digested with BglI and BglII, which have single cutting sites in CTXΦ at *rstR*^{ET}/*rstR*^{Env} and *zot*, respectively, showed identical RFLP patterns for all *V. mimicus* strains. Size-wise comparative analyses of the bands detected by hybridization, using different probes, of the enzyme-digested gDNA revealed similar results, i.e., the presence of two copies of pre-CTXΦ^{Env} prophages and a single CTXΦ^{ET} prophage, in all six strains of *ctx*$^{+}$ *V. mimicus*. Probing with *ctxA* and *rstR*^{Env} of the BglI-digested gDNA

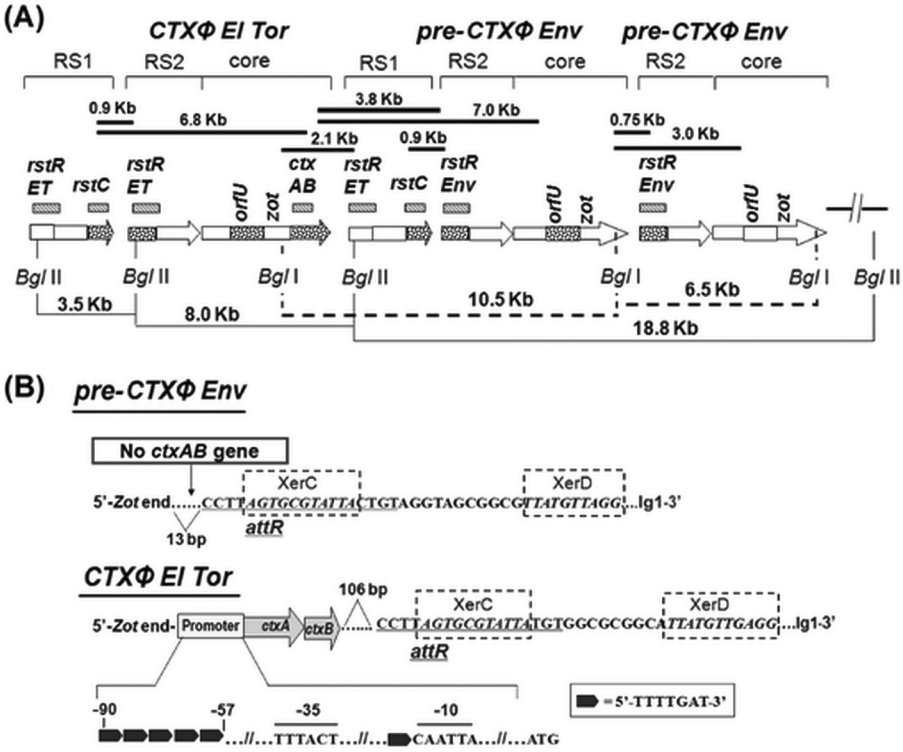

FIG 3 Organization of CTXΦ$^{El\ Tor}$, RS1, and pre-CTXΦ^{Env} in *V. mimicus* strains. (A) Filled bars indicate the PCR arrays used to check probable locations of genes, and the sizes of PCR products are given at the top. Hashed bars indicate the genetic regions (names mentioned at the top) used as probes for Southern hybridization after restriction digestion with BglI or BglII enzymes; arrows indicate RS1, RS2, or core prophage data where dotted regions were analyzed by sequencing. Lines (filled and dotted) at the bottom show the distances between specific genetic locations determined by Southern hybridization analysis of the BglI- or BglII-digested genomic DNA performed using specific probes. (B) Signature sequences in the flanking region of pre-CTXΦ^{Env} and CTXΦ$^{El\ Tor}$ in *V. mimicus*. The *ctxAB* promoter of CTXΦ$^{El\ Tor}$ contains 5 heptamer (TTTTGAT) repeats, shown by filled black arrows, which is characteristic of classical type *ctxAB*. The phage integration site of the CTXΦ$^{El\ Tor}$ in *V. mimicus*, the *attR* sequence, followed by XerC and XerD binding sites, starts at 106 bp downstream of *ctxAB* gene, which is similar to the reference El Tor strain, N16961, of *V. cholerae*. However, the phage integration site, characterized by these signature sequences, of pre-CTXΦ^{Env} in *V. mimicus* starts at 13 bp downstream of the *zot* gene.

generated a single positive band (ca. 10.5 kb) and two positive bands (ca. 6.5 and 10.5 kb), respectively. These results indicated the presence of one copy of CTXΦ containing *ctxAB*, followed by a pre-CTXΦ^{Env} (lacking *ctxAB*) with an adjacent RS1 and pre-CTXΦ^{Env} without RS1 (Fig. 3 and Fig. S3). Probing with *rstR*^{Env} and *rstR*^{ET} of the BglII-digested gDNA resulted in one (ca. 18.8 kb) and three (ca. 3.5, 8.0, and 18.8 kb) positive bands, justifying the adjacent locations of one RS1 followed by two pre-CTXΦ^{Env} prophages, along with the preceding occurrence of another RS1 and El Tor type full-length CTXΦ containing *ctxAB*. Hybridization with *rstC* probe justified the presence of two copies of the RS1 element, one before the CTXΦ^{ET} and the other preceding the adjacent pre-CTXΦ^{Env}. However, there was no RS1 element between the two adjacent CTXΦ^{Env} prophages. Taking the data together, an array of RS1–CTXΦ^{ET}–RS1–pre-CTXΦ^{Env}–pre-CTXΦ^{Env} was deduced from the Southern hybridization analysis.

To verify the hybridization results, PCR arrays were performed using the allele-specific forward and reverse primers with multiple combinations of *rstC*, *rstR*, *ctxAB*, and *orfU* genes (Fig. 3). All six *ctx*$^{+}$ *V. mimicus* strains yielded similar amplicons after PCR performed using primers specific for different regions of the CTX element. Size-wise comparisons of the PCR amplicons were in concordance with the published genetic organization of El Tor strains of *V. cholerae*. The results of PCR walking were in concordance with hybridization results, confirming the presence of the RS1 element *rstR*^{ET} in RS2 of the CTXΦ carrying *ctxAB* and of the *rstR*^{Env} allele in RS2 of a pre-CTXΦ

element(s), which lacked the *ctxAB* operon (Fig. S2; see also Fig. S3). The flanking sequences of CTXΦ^{ET} harbored both the RS1 and RS2 elements, similarly to the reference *V. cholerae* O1 El Tor strain N16961. Sequencing analysis of several core and intergenic regions of the CTX element (Fig. 3), confirmed the tandem presence of three copies of the CTX element, including one intact CTXΦ^{ET} copy and two pre-CTXΦ^{Env} prophages lacking *ctxAB*.

Genomic signatures in *ctxAB* promoter and intergenic sequences. The sequential integration of pre-CTXΦ^{Env} (lacking *ctxAB*) and CTXΦ^{ET} in *V. mimicus* strains prompted sequencing analysis of intergenic regions, particularly of the *ctxAB* promoter and the prophage flanking regions, to reveal genomic signatures associated with their lysogenic transformation. Forward and reverse primers of the adjacent genes, i.e., the *zot*, *ctxA*, *ctxB*, and *rstR*^{ET} genes for El Tor CTX prophage and the *zot* and *rstR*^{Env} genes for environmental pre-CTX prophage, amplified the desired portions of *ctxAB* promoter and intergenic regions. Sequencing analysis of the El Tor CTX prophage showed that the promoter at the 5′ upstream region of *ctxAB* contained 5-heptamer (TTTTGAT) repeat spanning the sequence from −90 to −57 bp, which is a characteristic of the classical type *ctxAB* promoter, while the RNA polymerase binding sites at −35 bp (TTTACT) and −10 bp (CAATTA) were conserved (Fig. 3). The 3′ end of *ctxAB* was characterized by *attR* sequences coupled with the XerC and XerD binding sites for CTXΦ integration, which started 106 bp downstream, similarly to N16961, the reference El Tor strain of *V. cholerae*. On the other hand, the 3′ end of pre-CTX^{Env} prophage was characterized by a 13-bp gap between the *zot* (the last gene of the phage core region) and *attR* sequences, followed by XerC and XerD binding sites (Fig. 3).

PCR, sequencing, and phylogenetic analysis of *tcpA* and *toxT*. PCR performed using a forward primer (primer tcpA-F [Table 3]) from the starting part of the 5′-terminal conserved region and a reverse primer for the El Tor type or classical type of *tcpA* did not yield any amplicon. However, using the forward primer tcpA-F and a reverse primer for *tcpQ* (tcpQ-R) yielded a 2.1-kb product, reconfirming the results of a previous study (8), for all of the *ctx*$^{+}$ *V. mimicus* strains. DNA sequencing showed that all of the strains had identical *tcpA* genes, and BLAST search analysis revealed the occurrence of a new *tcpA* allele, designated *tcpA*$^{Env\_Vm}$. Phylogenetic analysis revealed that this gene had homology of between 69.3% and 96.4% to other reported *tcpA* sequences and could be categorized into a novel cluster clearly separated from other major *tcpA* clusters, including the classical, El Tor, Nandi, and Novais types. The novel *tcpA*$^{Env\_Vm}$ gene found in *V. mimicus* strains showed the closest similarity to a couple of *V. cholerae* non-O1/non-O139 strains isolated in India and the United States and also to a *V. mimicus* strain (GenBank accession no. NZ_ACYV01000002) isolated from the USA (Fig. 4). Most of the diversities observed among the *tcpA* alleles were in the carboxy-terminal half, but the amino-terminal region was almost completely conserved among the compared sequences. Comparative sequence analysis performed with the reference classical and El Tor strains of *V. cholerae* O1 showed that the *tcpA*$^{Env\_Vm}$ gene had 74% homology at the DNA level to that of the El Tor (N16961) and classical (O395) *tcpA* genes, with 40 and 43 substitutions, respectively, among 224 deduced amino acids of the *tcpA* gene (Fig. 4; see also Fig. S4). The Nandi and Novais TcpA types differed by 15 and 45 amino acid residues in comparison to that of the *V. mimicus* of this study. Phylogenetic analysis also observed high TcpA sequence homology of one *V. mimicus* strain isolated from Brazil and another strain from China to the canonical TcpA of classical and El Tor O1 *V. cholerae*, respectively. However, those classical and El Tor TcpA types of *V. mimicus* had 40 and 42 differences in amino acids, respectively, from TcpA^{Env_Vm}.

Similarly to the results seen with *tcpA* amplification, PCR using the conventional primers for *toxT* did not produce any amplicon for the environmental *V. mimicus* strains of this study. However, application of newly designed primers (Table 3), considering variations in classical, El Tor, and environmental types of *toxT*, successfully yielded a specific amplicon of this gene in the study strains. Sequencing results showed identical

TABLE 3 Primers and probes used in this study

Target[a]	Primer ID[b]	Sequence (5′–3′)	Amplicon (bp)/special fragment(s) in Fig. 3 (kb)	Purpose(s)[c]	Reference or source
ctxA	ctxA-F	ACAGAGTGAGTACTTTGACC	307 bp	PCR/CBH/Seq	57
	ctxA-R	ATACCATCCATATATTTGGGAG	307 bp/6.8 kb	PCR/CBH/Seq	57
ctxB	ctxB-F	GATACACATAATAGAATTAAGGAT	399 bp/3.8 kb, 7.0 kb	PCR/Seq	58
	ctxB-R	TTGCCATACTAATTGCGG		PCR/Seq	This study
	ctxB-com5-F (common)	ACTATCTTCAGCATATGCACATGG		MAMA PCR	This study
	ctxB-cla3-R (classical)	CCTGGTACTTCTACTTGAAACG	366 bp	MAMA PCR	47
	ctxB-e13-R (El Tor)	CCTGGTACTTCTACTTGAAACA	366 bp	MAMA PCR	47
orfU	orfU-F	CGTCACACCAGTTACTTTTCG	1,072 bp	PCR/Seq	43
	orfU-R	AGAATGTACGCCATCGC		PCR/Seq	43
	orfU-R1	CGAAAAGTAACTGGTGTGACG	7.0 kb, 3.0 kb	PCR/Seq	This study
zot	zot-1	GGCTTAAACCTTGAACGC	1,036 bp	PCR	This study
	zot-2	AACCCCGTTTCACTTCTAC		PCR	This study
	zot-F1	ATGAGTTTGAAACCATACACTTT	2.1 kb, 0.75 kb, 3.0 kb	PCR/Seq	This study
rstC	rstC-F	ATGAGTTTGAAACCATACACTTT	225 bp/0.9 kb, 6.8 kb	PCR/CBH/Seq	17
	rstC-R	TTACAGTGATGGATCAGTCAAT	225 bp	PCR/CBH/Seq	17
rstR	rstR-R (common)	TCGAGTTGTAATTCATCAAGAGTG		PCR/CBH/Seq	20
	rstR (classical)-F	CTTCTCATCAGCAAAGCCTCCATC	474 bp	PCR	20
	rstR (El Tor)-F	GCACCATGATTTAAGATGCTC	501 bp	PCR/CBH/Seq	20
	rstR (Calcutta)-F	CTGTAAATCTCTTCAATCCTAGG	313 bp	PCR	20
	rstR (Environment)-F	GTTAACGCTTCAAGCCTG	372 bp	PCR/CBH/Seq	This study
	rstR (El Tor)-R1	GAGCATCTTAAATCATGGTGC	0.9 kb, 2.1 kb	PCR/Seq	This study
	rstR (Environment)-R1	CAGGCTTGAAGCGTTAAC	0.9 kb, 3.8 kb, 0.75 kb	PCR/Seq	This study
tcpA	tcpH1-F	AGCCGCCTAGATAGTCTGTG	1,324 bp	PCR/Seq	45
	tcpA4-R	TCGCCTCCAATAATCCGAC		PCR/Seq	45
	tcpA-F	CACGATAAGAAAACCGGTCAAGAG	2,108 bp	PCR/Seq	25
	tcpQ-R	GAGGACTGTTCTGCAAATCTGCTCAT		PCR	34
	tcpA (classical)-R	TTACCAAATGCAACGCCGAATG		Seq	This study
	tcpA (El Tor)-R	CGAAAGCACCTTCTTTCACACGTTG		Seq	This study
toxT	toxT-R	CCATGAATGTAGCACCAAG		PCR/Seq	This study
	toxT-F	CTTGTCTATTGTTCGTAAAGTG	834 bp	PCR/Seq	This study
	toxT-F2	CTGATGATCTTGATGCTATG	298 bp	PCR/Seq	This study
TLC	tlc-F	GGGAATGTTGAGTTCTCAGTG	1,548 bp	PCR	6
	tlc-R	GTTGCGAAGTGGATTTTGTG		PCR	6
RTX	rtx-F	CACTCATTCCGATAACCAC	1,366 bp	PCR	6
	rtx-R	GCGATTCTCAAAGAGATGC		PCR	6
T3SS-2	vcsN2-F	CAACACCTTCAAAGCCTTG	848 bp	PCR/CBH	This study
	vcsN2-R	GCGAGCTCCAATTGAAAC		PCR/CBH	This study
NAG-ST	stn-F	GAGAAACCTATTCATTGC	216 bp	PCR/CBH	59
	stn-R	GCAAGCTGGATTGCAAC		PCR/CBH	59
VSP-I	VC0175F2	TGAGGGCTGCTGAATAAG	689 bp	PCR/CBH	This study
	VC0175R2	TTGGCTCTGGTGTAAAGG		PCR/CBH	This study
	VC0183F2	AATACCACAAAGGACGCAC	687 bp	PCR/CBH	This study
	VC0183R2	TGGCCTAACCATAAGCAG		PCR/CBH	This study
VSP-II	VSPII LA F2	CGCACATACTCTTTGGTGGCATCAG	10,091 bp	PCR/CBH	This study
	VSP LA R2	ACTCTCTCTGATGGTGATGGCCTTC		PCR/CBH	This study
chxA	chxAF1	GTCGAAGATGAGTTAAACAT	1,904 bp	PCR/CBH	13
	chxAR1	TTATTTCAGTTCATCTTTTCGC		PCR/CBH	13

(Continued on next page)

TABLE 3 (Continued)

Target[a]	Primer ID[b]	Sequence (5′–3′)	Amplicon (bp)/special fragment(s) in Fig. 3 (kb)	Purpose(s)[c]	Reference or source
VSP-I	VC0175F2	TGAGGGCTGCTGAATAAG	689 bp	PCR/CBH	This study
	VC0175R2	TTGGCTCTGGTGTAAAGG		PCR/CBH	This study
	VC0183F2	AATACCACAAAGGACGCAC	687 bp	PCR/CBH	This study
	VC0183R2	TGGCCTAACCATAAGCAG		PCR/CBH	This study
VSP-II	VSPII LA F2	CGCACATACTCTTTGGTGGCATCAG	10,091 bp	PCR/CBH	This study
	VSP LA R2	ACTCTCTCTGATGGTGATGGCCTTC		PCR/CBH	This study
chxA	chxAF1	GTCGAAGATGAGTTAAACAT	1,904 bp	PCR/CBH	13
	chxAR1	TTATTTCAGTTCATCTTTTCGC		PCR/CBH	13
recA	Vm-recA-F	CTGGGTGTTAATATCGATGAG	73 bp	RT-PCR	This study
	Vm-recA-R	TCACAAATTTCTAGTGCTTG		RT-PCR	This study
	Vm-recA-P	CTACTGGTTTCTCAGCCAGATACCGGTGA		RT-PCR	This study
toxR	Vm-toxR-F	TCCGATTAGGCAGTAACGAAA	83 bp	RT-PCR	This study
	Vm-toxR-R	ATGCAAATCGTTGCGAGAAAC		RT-PCR	This study
	Vm-toxR-P	TCGAATTCTTTGGCTGCTTGCTCAGC		RT-PCR	This study
toxS	Vm-ToxS-F	TGGCAATCGAAGATGGTTTCA	76 bp	RT-PCR	This study
	Vm-ToxS-R	ACATCAACACGGCTCAATGG		RT-PCR	This study
	Vm-ToxS-P	TGATCAAAACCAAGAGTAACAGTCCAGCA		RT-PCR	This study
hns	Vm-hns-F	GCTTATTTCTGCACTTTCAGG	85 bp	RT-PCR	This study
	Vm-hns-R	GTCGATGTACTTGTATTTCGC		RT-PCR	This study
	Vm-hns-P	ACTAAAGCAAAAGGCAAACGTGCTCCTCG		RT-PCR	This study
tcpA	Vm-tcpA-F	GCTCAGCGTGCGATTGACT	76 bp	RT-PCR	This study
	Vm-tcpA-R	GAGTAAGCGACACTTGGATTG		RT-PCR	This study
	Vm-tcpA-P	ATGACCAAGGCTGCGCAAAATCTCA		RT-PCR	This study
toxT	Vm-toxT-F	CGAGATTCTAGTTCTTTTTTCAAAACC	123 bp	RT-PCR	This study
	Vm-toxT-R	TGATGCTATGGAGAAAATATCATGTT		RT-PCR	This study
	Vm-toxT-P	TAATTCATCACAAACATCAGACCAACGCCA		RT-PCR	This study
ctxA	ctxA-F	GGAGGGAAGAGCCGTGGAT	66 bp	RT-PCR	49
	ctxA-R	CATCGATGATCTTGGAGCATTC		RT-PCR	49
	ctxA-P	CATCATGCACCGCCGGGTTG		RT-PCR	49
tcpP	tcpP-F	TGGTACACCAAGCATAATACAGACTAAG	100 bp	RT-PCR	49
	tcpP-R	AGGCCAAAGTGCTTTAATTATTTGA		RT-PCR	49
	tcpP-P	TACTCTGTGAATATCATCCTGCCCCCTGTC		RT-PCR	49
tcpH	tcpH-F	GCCGTGATTACAATGTGTTGAGTAT	82 bp	RT-PCR	49
	tcpH-R	TCAGCCGTTAGCAGCTTGTAAG		RT-PCR	49
	tcpH-P	TCAACTCGGCAAAGGTTGTTTTCTCGC		RT-PCR	49

[a]"T3SS-2" and "NAG-ST" indicate type III secretion system 2 and heat-stable enterotoxin of *V. cholerae*, respectively.
[b]"F," "R," and "P" indicate forward primer, reverse primer and probe, respectively. Gene names are indicated in the primer designations.
[c]"CBH" and "Seq" indicate colony blot hybridization and sequencing analysis, respectively.

levels of sequence homology of *toxT* in all the environmental *V. mimicus* strains. Comparative analysis identified the presence of a new allele with several unique substitutions and 76.9% to 78.0% homology among the deduced amino acid residues in comparison to the canonical *toxT* gene of the classical and El Tor *V. cholerae* strains (Fig. S5). Higher diversity was observed in the amino-terminal half of ToxT sequences than was seen in those of the environmental *V. mimicus* and *V. cholerae* O1 strains. Phylogenetic analysis clearly differentiated the *toxT* genes into two major clusters, one including the usual *toxT* gene commonly found in epidemic *V. cholerae* O1 strains and the other comprising the variant *toxT* gene identified in this study and in several *V.*

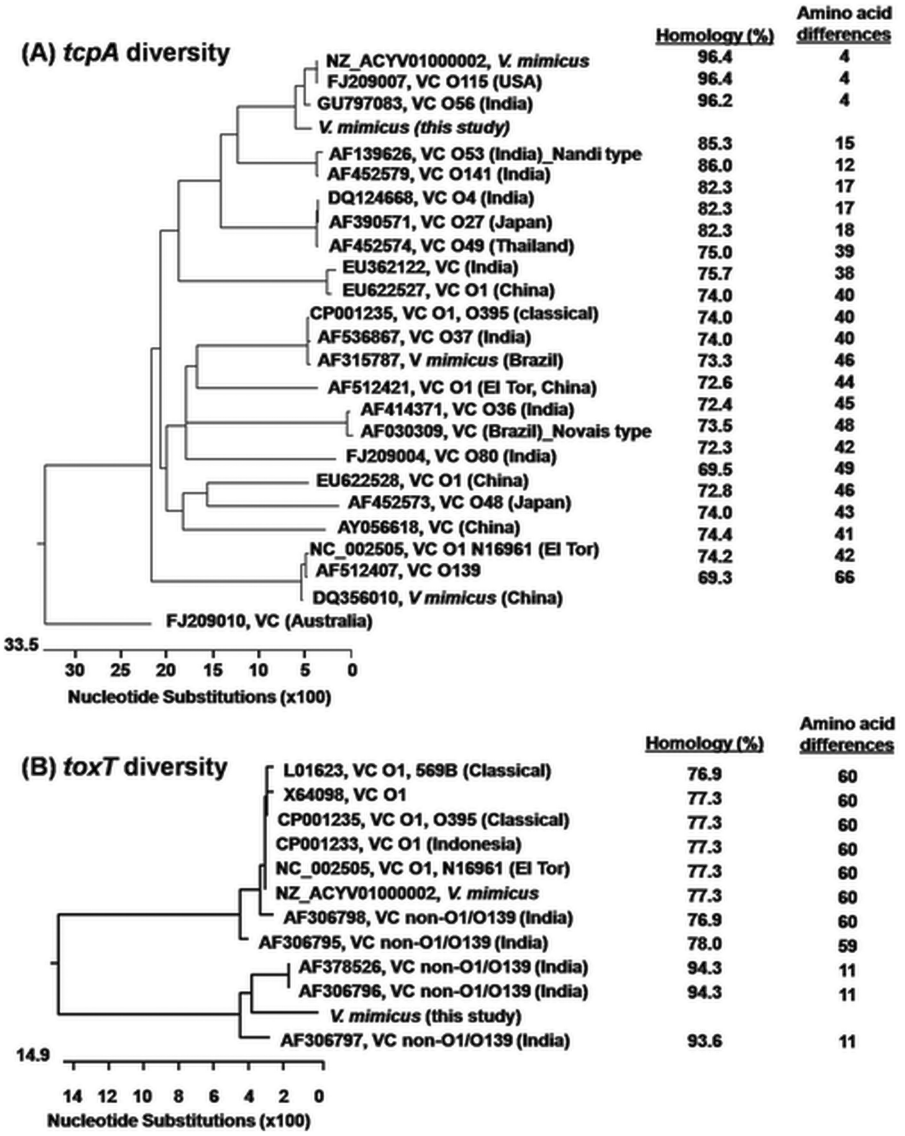

FIG 4 Genetic relatedness of *tcpA* and *toxT* genes among strains of *V. cholerae* and *V. mimicus* of different serogroups. (A) The novel *tcpA* gene of *V. mimicus* of this study did not cluster in classical strains, El Tor strains, or other types of strains but formed a separate clade showing closeness to strains of serogroups O56 and O115 of *V. cholerae*. (B) The novel *toxT* gene of *V. mimicus* of this study did not group into the major cluster comprising the *toxT* genes of *V. cholerae* O1 classical, El Tor, O139, and non-O1/non-O139 strains or of other *V. mimicus* strains but grouped into a separate cluster with atypical *toxT* genes reported in a few non-O1/non-O139 strains of *V. cholerae*.

cholerae non-O1/non-O139 strains from India (Fig. 4). However, the variant ToxT present in environmental *V. mimicus* strains was novel in terms of the acquired differences in 11 amino acid residues in comparison to that of the non-O1/non-O139 *V. cholerae* strain in the same phylogenetic cluster and to 59 to 60 amino acid residues with the canonical ToxT found in classical and El Tor *V. cholerae* O1.

CT production capacity and virulence potential. All the environmental *V. mimicus* strains showed identical patterns for the major virulence-related genes, including those of the predicted amino acid sequences in CTX prophages and the TCP island, which indicated their probable functional capability to produce CT and virulence-related proteins. Therefore, bead enzyme-linked immunosorbent assays (bead-ELISA) were carried out under established conditions for both the El Tor and classical strains of *V. cholerae* O1 to check the functional CT production capacity and its variations, if any,

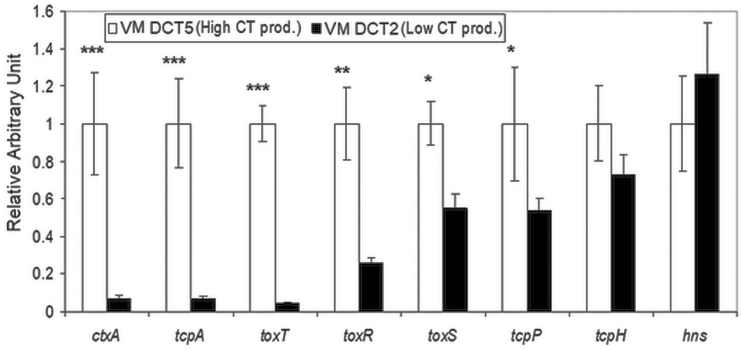

FIG 5 Variation in mRNA transcription levels of virulence genes and regulated genes between high-CT-producing and low-CT-producing strains of *Vibrio mimicus*. Transcriptional levels of various virulence-related genes were analyzed by qRT-PCR. The relative transcriptional level of each gene was normalized with the housekeeping *recA* gene. The mRNA transcription level of each gene in a low-CT-producing strain was compared with that of a high-CT-producing strain. The transcriptional level of each virulence-related gene of the high-CT-producing strain was arbitrarily assigned a value of 1 (relative arbitrary unit). Statistically significant differences were calculated using the two-sample *t* test. A *P* value of <0.05 was considered significant (***, $P < 0.005$; **, $P < 0.01$; *, $P < 0.05$).

among the environmental *V. mimicus* strains. Results showed that the CT production capacities differed among the environmental *V. mimicus* strains and were higher under the *in vitro* conditions favorable for the classical strains (LB medium, pH 6.6, 30°C) than under El Tor conditions for *V. cholerae* strains (AKI medium [1.5% Bacto peptone, 0.4% yeast extract, 0.5% NaCl, 0.3% $NaHCO_3$], pH 7.4, 37°C). Of the six *V. mimicus* strains, one strain (*V. mimicus* DCT5) showed high CT production capacity (110 and 30 ng ml^{-1} in LB and AKI, respectively) whereas the toxin production was very low (0.1 to 0.5 ng ml^{-1}) in others (Table 1).

Suckling mouse assay (SMA)-based *in vivo* experiments produced results in congruence with the CT production capacity for the *V. mimicus* strains (Table 1). Both live cells (10^6 to 10^7 CFU) and culture filtrates of *V. mimicus* strain DCT5 producing high CT levels induced fluid accumulation and diarrhea in all the experimental mice and hence were revealed to be enterotoxigenic. The SMA score, representing the fluid accumulation ratio, ranged between 0.083 and 0.090 (0.087 ± 003) for the high-CT-producing *V. mimicus* strain DCT5. However, none of the experimental mice exhibited diarrhea when low-CT-producing *V. mimicus* strain DCT2 was administered at a normal dose (10^7 CFU) or even when it was administered at a higher dose ($>5 \times 10^9$ CFU). The fluid accumulation ratio shown by this strain with attenuated CT production ranged between 0.065 and 0.070 (0.0068 ± 002), which was similar to the range seen with the negative control (0.062 ± 002) (Table S1).

Transcriptional analysis of genes associated with CT production. According to the results of bead-ELISA, the optimum culture condition for CT production, i.e., the classical type condition using LB medium, was selected for transcriptional analysis of *ctxAB* and its known regulatory genes by quantitative reverse transcription-PCR (qRT-PCR) in the high-CT-producing (*V. mimicus* DCT5) and low-CT-producing (*V. mimicus* DCT2) environmental *V. mimicus* strains used in SMA *in vivo* experiments. As expected, a significantly lower level of transcription of *ctxA* was observed in the low-CT-producing strain than in the high-CT producer. Similarly, significant low-level transcription of *tcpA* and *toxT*, which are known to directly interact with CT production, was also observed. In checking the transcription of other genes in the ToxR regulon influencing CT production, high and low levels of transcription of *ctxA* were observed to be correlated with the mRNA transcription of *toxR*, *toxS*, and *tcpP* (Fig. 5). In the low-CT-producing strain, the levels of transcription of the *ctxA*, *tcpA*, and *toxT* genes were significantly lower by about 15-fold to 25-fold ($P < 0.005$) than those of the high-CT-producing strains. Similarly, *toxR* expression was also significantly (about 4-fold [$P < 0.01$]) lower, while both *toxS* and *tcpP* showed about 2-fold ($P < 0.05$)-lower transcription. In the

low-CT-producing strain, *tcpH* transcription was about 1.4-fold lower but the difference was not significant in comparison to the high-CT producer. On the other hand, an opposite trend was observed for *hns* transcription; the high-CT-producing strain showed about 1.3-fold-lower *hns* transcription than the low CT producer, although the difference was not significant.

DISCUSSION

Understanding the adaptive evolutionary mechanism of the CTXΦ and *ctxAB* genes encoding the cholera toxin (CT) is highly important because of its direct relation to severe diarrheal diseases such as cholera, which causes health hazards throughout the world. In this aspect, through acquisition of toxigenic *ctxAB* genes, *V. mimicus* might play a salient role in its maintenance and propagation in the natural environment. A previous investigation (8), suggesting a possible occurrence of atypical *tcpA* in these *ctx*$^+$ *V. mimicus* strains, prompted us to perform detailed characterizations (e.g., genotyping, sequence diversity, and transcriptional analysis) of genes of CTX prophage and ToxR regulon and to compare the characteristics of genomic relatedness, CT production *in vitro*, and virulence potential *in vivo* of these strains.

Novel *ctxAB* allele and multiple CTX prophages in environmental *V. mimicus* strains. Comparing the core and flanking regions of CTX prophage in *V. mimicus* with those of *V. cholerae* strains showed a lot of previously unidentified variation in amino acid residues. Remarkably, the novel *ctxB* variant (Table 2), designated genotype 14, in the *V. mimicus* strains is distantly related to El Tor genotype 3 but is more closely related to the classical genotype 1 and Haitian genotype 7, the predominant traits of *V. cholerae* hybrid strains associated with the recent cholera epidemics (2–4). The functional implications of these changes in *ctxAB* in *V. mimicus* are required to be investigated in detail, particularly in relation to virulence potential, e.g., the crystal structure of the variant CT (27), constructing mutant strains and verifying the possible impacts of the changes by *in vivo* experiments. On the other hand, comparison of the *orfU* genes of CTX prophage in *V. mimicus* strains could identify its close homology with that of the El Tor type, which is inconsistent with its reported affiliation with the classical clade of *V. cholerae* O1 (7). Nonetheless, several unique changes in the amino acid residues within the first two domains (D1 and D2) of three domains of *orfU* (28) indicated the ongoing evolution of CTX prophage in *V. mimicus* in parallel to those of the epidemic *V. cholerae* O1. These polymorphic residues in *orfU* (gIII^{CTX}) most likely interact with the periplasmic protein, TolA, and with "adsorption" domains, associated with phage penetration (28).

The occurrence of a single-copy CTX prophage in the studied *V. mimicus* strains was claimed in a previous study, based on hybridization of gDNA restriction digestions with *ctxA* probe (8). However, our results obtained by genome walking through a series of hybridization and PCR assays demonstrated that the *V. mimicus* strains actually contain one mature El Tor type prophage (CTXΦ^{ET}) with *ctxAB* and two environmental type pre-CTX prophages (pre-CTXΦ^{Env}) without *ctxAB*. The existence of pre-CTXΦ has been reported for only a very few strains of *V. cholerae*, including the epidemic O1/O139 strain and also non-O1/O139 strains (19, 22, 25, 29). Integration of at least two types of CTXΦ (El Tor and environmental) within the genome of *V. mimicus* is an interesting and novel observation. In *V. cholerae* strain N16961, the reference El Tor strain, the phage integration site, characterized by the *attR* sequence followed by XerC and XerD binding sites, starts at 106 bp downstream of *ctxAB* (30). That study observed a similar location for the integration site of CTXΦ^{ET} but a different intergenic location of *attR*-XerC-XerD for pre-CTXΦ^{Env}. The occurrence of the RS1 element in the *V. mimicus* strains follows the evolutionary trait of the El Tor strains of *V. cholerae*. Acquisition of RS1 may not only increase CTXΦ production, with a possible influence on *ctxAB* transcription, but also promote genomic diversity by the loss of CTX prophage and lysogenic immunity to make room for new CTX prophage to be integrated (18, 29, 31). In comparison to the canonical El Tor type strains, the hybrid El Tor strains with the classical *ctxB* genotype are considered to be more virulent than the El Tor CT producer (32). The acquisition of

hybrid CTXΦ^{ET} by the *V. mimicus* strains might have equipped them with greater evolutionary fitness, since these pathogenic strains can utilize the chance of becoming selectively enriched in the intestine of humans and animals (33).

Diverse TCP and ToxT alleles in *V. mimicus* strains. Not only the CTX elements but also the TCP genes in *V. cholerae* can be mobilized by generalized transduction (34). The sequence of the *tcpA* locus in the TCP element is known to be more divergent than those of other loci in the VPI (35). Similarly, we have observed a high diversity in *tcpA* sequences by phylogenetic analysis, which is in congruence with previous studies (36, 37). Notably, the environmental *V. mimicus* strains contain a novel allele of *tcpA*, identified as *tcpA*$^{Env\_Vm}$, with ca. 70% to 74% homology at nucleotide level compared to the reference El Tor and classical strains of *V. cholerae* O1. The progenitors of these *V. mimicus* strains might have acquired this *tcpA* genotype from *V. cholerae* non-O1/non-O139 strains of a particular phylogenetic clade, including the O56 and O115 serogroups, and/or vice versa (Fig. 4). This observation is not coherent with the previously reported *V. mimicus tcpA* genotypes, clustered to the phylogenetic clades comprising the canonical classical and El Tor strains of *V. cholerae* O1 (36). Most likely, this diversity is a reflection of diversifying selection with respect to CTXΦ susceptibility as part of the ongoing adaptive evolution among potentially pathogenic *Vibrio* populations of this kind. Similar reasons may explain the occurrence in studied *V. mimicus* strains of a novel *toxT* allele, affiliating with the atypical *toxT* gene of certain non-O1/non-O139 strains but not the canonical *toxT* of epidemic O1 classical and El Tor strains of *V. cholerae* (25).

Comparative analysis of *tcpA* sequences has clearly identified a high substitution rate in the carboxy-terminal half, encoding the exposed part of the TCP pilus on the cell surface. Among the many differences between the novel *tcpA*$^{Env\_Vm}$ gene and the *tcpA*^{Cla} gene is the ca. 187 V>K substitution, which may influence pilus-mediated autoagglutination (38). In the case of *toxT*, the diversity in amino acid residuals in comparison to the reference strain was higher in the amino-terminal half, which is in accordance with a previous study (25). The relatively conserved carboxy-terminal half is known to determine the specificity of ToxT protein binding to DNA regulatory sites (25). Apart from acting as a virulence factor, TCP may also aid in environmental persistence, e.g., of biofilm formation on aquatic particles and of organisms, particularly, chitinous zooplankton (39). The occurrence of a new variant *tcpA* gene, with possible alterations in cell surface epitopes, among the toxigenic *V. mimicus* strains of the present study might be have been a consequence of an adaptive evolutionary response to the changes in environmental niche.

Variation in CT production and virulence potential and its regulatory framework in *V. mimicus*. In the case of *V. cholerae*, strains producing a concentration of CT of at least ~20 ng ml^{-1} are known to cause fluid accumulation or diarrhea in experimental animal (32). Most of the *V. mimicus* strains did not cause fluid accumulation in sucking mice, in concordance with the very low level of CT production (<0.5 ng ml^{-1}) seen under *in vitro* growth conditions. Yet these strains are potentially toxigenic, as reflected in one of the *V. mimicus* strains, with identical virulence genotypes but producing a high amount (>100 ng ml^{-1}) of CT and diarrhea *in vivo*. We also cannot rule out the possibility that the experimental conditions used in this study may not be optimal for CT production in *V. mimicus* strains and need to be further investigated using different culture conditions and growth media. The absence of any other potential virulence factors, e.g., the TTSS, NAG-ST, ChxA, and RTX, indicates that the observed enterotoxicity in mice intestine is due to CT produced by the environmental *V. mimicus* strains. However, detailed investigations, including understanding the role of intestinal receptors (other than GM1) of CT and the intestinal colonization capacity of these *V. mimicus* strains containing a new variant of *tcpA*, are required to decipher the virulence mechanism triggering diarrhea in mouse (40, 41).

Despite the presence of CTXΦ and the TCP element, the variation in CT production in *V. mimicus* strains is likely influenced by other genetic factors; e.g., the expression of

CT and TCP in *V. cholerae* is activated by ToxT, which is regulated by the TcpP-TcpH-ToxR-ToxS complex (24). In the case of the high-CT-producing *V. mimicus* strain, higher transcription of *ctxA* in conjunction with that of *tcpA* and *toxT* and the upstream-regulatory genes *toxR* and *toxS* corroborates the known ToxT-ToxR-mediated genetic regulation influencing CT production in *V. cholerae*. In addition, the histone-like nucleoid structuring protein (H-NS) encoded by *hns*, a global prokaryotic gene regulator, has been shown to repress the transcription of virulence genes, including *toxT*, *ctxAB*, and *tcpA* in *V. cholerae* (42). However, the variation in CT production in *V. mimicus* strains is not influenced by the H-NS since its transcription did not show a considerable change in parallel to that of *ctxAB*. The ToxR regulon is thought to be controlled by environmental stimuli, such as temperature, pH, and osmolarity (24). Hence, understanding the precise genetic and physiological mechanisms behind the variations in the level of CT production in *V. mimicus* requires more-extensive research beyond the scope of this study.

Probable role of *V. mimicus* in the evolution of CTXΦ. In the *V. mimicus* strains, the presence of the recombinase XerC and XerD binding sequences at both ends of the pre-CTXΦ^{Env} and CTXΦ^{ET} prophages support the concept of phage-mediated integration events of these external genetic elements (23). Pathogenic *V. cholerae* strains are thought to have evolved from their nonpathogenic progenitors first through acquisition of *tcpA* and other genes of VPI and then through integration of CTXΦ (43). On the other hand, special forms of the CTXΦ family, designated pre-CTXΦ, do not carry *ctxAB* but contain other genes considered to be CTXΦ precursors (6). The occurrence of RS1–CTX^{ET}–RS1–pre-CTX^{Env}–pre-CTX^{Env} in *V. mimicus* suggests their integration through stepwise horizontal gene transfers (HGTs) and recombination of phage genes, and these strains may be considered to be among the missing evolutionary links for the diverse arrays of multiple alleles of CTX^{ET}, pre-CTX^{Env}, and RS1 reported to occur in the O1 and non-O1/O139 strains of *V. cholerae* (19–22, 29). The presence of tandem copies of CTX and RS1 phages along with the novel types of *ctxAB*, *tcpA*, *toxT*, and *orfU* indicates that CTX prophages in the *V. mimicus* genome might have evolved independently of the seventh-pandemic El Tor clones, probably through independent integration of pre-CTXΦ^{Env}, in duplicate, and then of a primeval CTXΦ^{ET} (19). This proposition is in congruence with the absence of other hallmark factors of the El Tor strains, including VSP-I and VSP-II gene clusters, and also the RTX and TLC elements (11, 21), in these *V. mimicus* strains. Several studies comparing genome sequences have also indicated horizontal transfer of virulence-related genes in *V. mimicus* from an uncommon clone of *V. cholerae* rather than from the seventh-pandemic strains (9, 44). This is further supported by the existence in the *ctxAB* promoter region of *V. mimicus* strains of five heptamer (TTTTGAT) repeats, a characteristic genomic signature of the classical O1 strain isolated during the 1960s, while the El Tor O1 strains, isolated from the 1970s onward, contained four heptamer repeats (30).

The evolutionary success or failure of a new allele depends on numerous factors, e.g., the consecutive direction of gene flow, precursor-product relationships and influences of regulatory molecular-genetic processes during evolution, and the ecological fitness of the host bacterium, which is very difficult to predict or decipher. Nonetheless, the adaptive survival of particular *ctx*$^+$ *V. mimicus* strains in the estuarine environment is indicated in their isolation during different months of a given year. These strains have been observed to be clonally related, which suggests their probable origin from a common ancestor. However, as reflected by their variable antimicrobial resistance traits and differentiation into several PFGE subtypes, *V. mimicus* strains of this kind are prone to genomic modifications, some of which may aid in their ecological fitness. The probable influence of environmental *V. mimicus* on the ongoing population shift of typical El Tor strains to hybrid El Tor strains carrying classical and variant type *ctxB* cannot be dismissed. Through acquisition of pre-CTXΦ, particular *tcp*$^+$ strains of *V. mimicus* probably serve as a cryptic but important natural reservoir of the CTXΦ and TCP and related virulence genes.

Conclusion. It can be inferred that certain clonally related environmental *V. mimicus* strains can act as reservoir of variant *ctxB* genes, designated genotype 14, which is phylogenetically closer to currently predominant genotypes 1 and 7 associated with cholera outbreaks worldwide. This report provides molecular insight into the virulence potential of *ctx*$^+$ *V. mimicus* strains, which could potentially serve as reservoirs of novel or variant types of not only *ctxAB* but also *tcpA*, *toxT*, and *orfU*. The genomic contents of tandemly arranged multiple pre-CTXΦ^{Env} types and a CTXΦ^{ET} with novel classical type *ctxAB* probably act as salient raw materials for the natural recombination events driving the evolution of virulence genes related to CT production. Though CT production in some examples of environmental *V. mimicus* strains of this kind can be naturally attenuated, the strains might be toxigenic under favorable conditions and might be able to instigate cholera-like diarrhea. The variation in CT production capacity in *V. mimicus* is partially explained by the coordinated differential transcription of several genes within the ToxR-ToxT regulatory cascade. The cryptic existence of the virulence genes related to CT production in *V. mimicus* genome points out an unnoticed event in the evolutionary pathway of CTXΦ ecology and cholera epidemiology. Systematic environmental surveillance of nonepidemic strains, including *V. mimicus* and *V. cholerae*, and associated detailed investigations of the genetic and functional diversities of genes influencing CT production and virulence potential in different hosts and under different environmental conditions would allow us to improve understanding the evolution of new variant *ctx* elements and of CTXΦ as well as of the genes that regulate them.

MATERIALS AND METHODS

Bacterial strains and their antimicrobial susceptibility. Six *ctx*$^+$ *V. mimicus* strains (Table 1) were obtained from the culture collection of the Environmental Microbiology Laboratory of icddr,b, Dhaka. These strains were isolated during the postmonsoon and early winter months in 2000 from the Karnaphuli River estuary, Bangladesh. The *ctx*$^+$ strains were screened from 1,600 presumptive *V. mimicus* colonies, grown on thiosulfate citrate bile salts sucrose (TCBS) agar after enrichment of environmental samples in alkaline-peptone-water (APW) (pH 8.0). All strains were grown in Luria-Bertani (LB) broth, and their identity was verified according to a standard protocol (45). Strains stored as glycerol stock at −80°C were grown in APW and subsequently on TCBS agar (Difco Laboratories, MI, USA), gelatin agar (Difco), and LB at 37°C whenever needed. Several reference strains of *V. cholerae* (i.e., N16961 and O395, representing the El Tor and classical biotypes, respectively; VCE233 and AS522, non-O1/non-O139 strains containing environmental and Kolkata type CTX prophages; SG6, a type III secretion system [TTSS]-positive non-O1/non-O139 strain; GP156, a *stn*-positive O1 El Tor strain; and C9, a *chxA*-positive non-O1/non-O139 strain) and *V. mimicus* ATCC 33653^T were used as controls. Each of the *ctx*$^+$ *V. mimicus* strains was examined for resistance to some commonly used antimicrobials (Table 1) to observe related phenotypic variations, if any. Antimicrobial resistance was determined by the disc diffusion method according to the Clinical and Laboratory Standards Institute (http://www.clsi.org) using Mueller-Hinton agar (Difco) and commercially available discs (Oxoid, Hampshire, England).

Pulsed-field gel electrophoresis (PFGE). PFGE was performed according to the Pulse Net USA protocol (https://www.cdc.gov/pulsenet/pathogens/pfge.html) with slight modifications. Briefly, freshly grown *V. mimicus* strains were embedded into 1% Seakem Gold agarose (Sigma-Aldrich, MO, USA) followed by lysis of the cells with 0.5 mg ml^{-1} proteinase K (P8044-5G; Sigma) and 1% sarcosine (Sigma) at 54°C for 1 h. Agarose blocks containing genomic DNA were digested with NotI and SfiI (TaKaRa Bio Inc., Otsu, Japan) (30 and 40 U, respectively) using appropriate buffer at 37°C for 3 h. DNA fragments were electrophoresed in 1% pulsed-field-certified agarose gel (Bio-Rad Laboratories, CA, USA) using a Chef Mapper (Bio-Rad). Gels were stained for 30 min and destained twice for 15 min each time, and images were captured using a Gel-Doc 2000 system (Bio-Rad). A lambda ladder (Bio-Rad) was used as a molecular mass standard. The PFGE fingerprints were analyzed by the use of Fingerprinting II software (Bio-Rad).

Colony blot hybridization of virulence-related genes. DNA probes for colony blot hybridization included the major toxigenic factors, e.g., cholera toxin (*ctxA*), zonula occludens toxin (*zot*; part of CTX phage), RS1 element (*rstC*), *Vibrio* seventh-pandemic island (including VSP-I and VSP-II, markers of the present pandemic O1 El Tor biotype), the TLC element, and other known virulence genes of *V. cholerae*, namely, *vcsN2*, *chxA*, *stn*, and *rtxA*, encoding the type III secretion system, cytotoxic cholix toxin, heat stable enterotoxin, and repeat in toxin, respectively. DNAs of reference *V. cholerae* strains and gene-specific primers were used as a template for PCR amplification of these genes (Table 3). PCR products were purified by standard methods and labeled by random priming with [α-^{32}P]dCTP (370 MBq mmol^{-1}) using a Multi-Prime DNA labeling system (GE Healthcare, Buckinghamshire, United Kingdom). Environmental *V. mimicus* strains were grown on nitrocellulose membrane, overlaid on LB agar at 37°C for 4 to 6 h, and subjected to colony blot hybridization following the procedure described by Yamasaki et al. (46). Radioactivity in the hybridized membrane was detected using a BAS FLA-3000 system (Fuji Film, Tokyo, Japan).

PCR-based typing of virulence genes and CTX phage element. Template DNA was prepared by the use of the standard boiling method and was stored at −30°C until use. MAMA-PCR (47) was employed to detect *ctxB* genotypes in *V. mimicus* strains to define their potential for classical or El Tor type CT production. The presence of the RS1 element was determined by *rstC* gene-based PCR (18). Genotypes of *rstR*, namely, classical, El Tor, Kolkata, and environmental genotypes, were also determined by PCR using a newly designed primer set for the environmental type and previously established protocols for others (20). The genotypes of *tcpA*, belonging to the VPI, were also checked by PCR using previously established methods (25). Details of the primers and PCR conditions for screening these genes are mentioned in Table 3.

Southern hybridization and PCR arrays to understand the genetic organization of CTXΦ. Southern hybridization analyses of BglI-digested and BglII-digested gDNA of *V. mimicus* strains were carried out with probes for selected virulence-related genes, including *ctxAB*, $rstR^{ET}$, $rstR^{Env}$, and *rstC*. Briefly, 5-μg aliquots of total gDNA were digested with the restriction enzymes using appropriate buffer and electrophoresed in 0.8% pulsed-field-certified agarose gel (Bio-Rad) using a Chef Mapper (Bio-Rad). Once separated, the gDNA fragments were subjected to Southern hybridization transfer and blotted onto nylon membranes (Hybond-*N*+; Amersham, GE Healthcare, Buckinghamshire, United Kingdom). The genomic blots were hybridized with the gene probes, labeled by random priming with [α-^{32}P]dCTP (370 MBq mmol^{-1}), and autoradiographed as described previously (13). In order to verify the genetic organization of CTXΦ and associated elements, a series of PCR arrays were performed using the forward and reverse allelic primers, with multiple combinations of genes *rstC*, $rstR^{ET}$, $rstR^{Env}$, *ctxAB*, and *orfU* as shown in Fig. 3 and the respective primers (Table 3).

Nucleotide sequencing and phylogenetic analysis of diversity of virulence genes. *V. mimicus* strains were subjected to nucleotide sequencing analysis for several target virulence genes of CTXΦ, including *ctxAB*, *orfU*, and *rstR*, and for associated flanking regions comprising *zot*, intergenic region 1 (ig-1) and ig-2, and TCP elements, namely, *tcpA* and *toxT*. Briefly, PCRs using primers (Table 3) targeting these virulence genes and flanking regions were conducted following standard protocols. The amplified products were purified using a QIAquick purification kit (Qiagen GmbH, Hilden, Germany), and then cycle sequencing was carried out using a BigDye Terminator v3.1 cycle sequencing kit according to the instructions of the manufacturer (Applied Biosystems, CA, USA). Afterwards, a further purification was done using CleanSEQ (Agencourt Bioscience, MA, USA), and nucleotide sequences were determined by the use of an ABI Prism 3100 Avant Genetic Analyzer (Applied Biosystems). The obtained gene sequences were assembled and aligned by the use of DNA Lasergene software (DNASTAR, WI, USA). Homology searching was performed using the BLAST program (http://blast.ncbi.nlm.nih.gov/Blast.cgi), and the nucleotide and deduced amino acid sequences were compared with those of published genes. A phylogenetic tree was constructed using the ClustalW algorithm to understand the genetic lineage and sequence diversity within the study strains and other representative sequences of the target genes of *V. mimicus* and *V. cholerae* published in GenBank. Representative sequences of the novel *ctxAB*, *tcpA*, *toxT*, and *orfU* genes in the *V. mimicus* strains of this study can be obtained from NCBI/DDBJ under accession no. LC427969, LC427970, LC427971, and LC427972, respectively.

Measuring CT production by bead enzyme-linked immunosorbent assay (bead-ELISA). The *ctx*-positive *V. mimicus* strains were grown in AKI medium (pH 7.4) and LB medium (L-broth) (Difco, KS, USA) (pH 6.6) for 12 h at 37 and 30°C, respectively, to compare their CT production levels under conditions favorable for the El Tor and classical strains of *V. cholerae* (48). Subsequently, the optical density at 600 nm (OD) nm of the bacterial cultures was adjusted to 1.0, followed by 100-fold dilution in the respective media and incubation under stationary and shaking conditions, for 4 h each, at 180 rpm (48, 49). The cell-free supernatant (CFS) of each culture was prepared by centrifugation at 12,000 × *g* for 10 min followed by filtration through a 0.22-μm-pore-size filter (Iwaki, Tokyo, Japan). The CFS from each culture was diluted 10, 100, and 500 times in 10 mM sodium phosphate buffer containing 100 mM NaCl (pH 8.0), and the level of CT produced was measured by bead-ELISA. Purified CT was obtained following the methodology described by Uesaka et al. (50) and was used as controls for known concentrations. Preparation of polyclonal rabbit antisera against CT, conjugation of Fab′ of antitoxin IgG with horseradish peroxidase, and estimation of the CT level secreted by each strain by bead-ELISA were done according to the method previously described by Oku et al. (51). All experiments were done in triplicate.

Detection of pathogenic potential *in vivo*. Two strains of *ctx*$^+$ *V. mimicus* showing similar PFGE pulsotypes but producing high and low CT levels, as detected by ELISA, were selected for evaluating enterotoxigenic potential *in vivo*. A suckling mouse assay (SMA) was performed using 3-day-old Swiss albino suckling mice according to standard procedures (52). Briefly, an aliquot (0.1 ml) of bacterial culture freshly grown in LB medium (as well as its filtrate [obtained using a 0.2-μm-pore-size filter]) was mixed with Evans blue (0.01% [wt/vol]) and intragastrically inoculated into each suckling mouse. A volume approximately equal to 10^7 CFU was inoculated as the normal dose; however, higher and lower doses were also administered for low-CT and high-CT producers, respectively. After 6 h of incubation, the intestines of the mice were removed, pooled, and weighed. The fluid accumulation score from the SMA was expressed as the ratio of the weight of the intestine to the remaining body weight, and a ratio of ≥0.08 was considered to represent a positive result. Culture filtrates of the reference strains of *ctx*$^+$ *V. cholerae* O1 (O395) and of *V. mimicus* lacking *ctx* (ATCC 33653^T) were used as positive and negative controls, respectively. The pathogenic potential of each strain was verified using five and three mice for live cells and culture filtrates, respectively.

RNA isolation and qRT-PCR assay. The *ctx*$^+$ *V. mimicus* strains, expressing high and low CT levels, were freshly grown to the mid-logarithmic phase (~10^8 CFU ml^{-1}) in LB medium under the classical condition (30°C) of CT production (48). Total RNA was extracted and purified using TRIzol reagent

(Gibco-BRL, NY, USA) according to the manufacturer's instructions. The qRT-PCR assay was carried out with the primers and probes for the appropriate genes, namely, *ctxA*, *tcpA*, *toxT*, *toxR*, *toxS*, *tcpP*, *tcpH*, and *hns*, which are known to regulate CT production, and a housekeeping *recA* gene as an internal control (Table 3) following the TaqMan probe method. Each probe was labeled with 6-carboxyfluorescein (FAM) and 6-carboxytetramethylrhodamine (TAMRA) as the 5′ reporter and 3′ quencher dyes, respectively. Reverse transcription was carried out for cDNA synthesis from an RNA template (1 μg) using a quick RNA-cDNA kit (Applied Biosystems) according to the manufacturer's instructions. Real-time PCR was carried out using the amplified cDNA and TaqMan Gene Expression master mix containing each set of primer and probe (Applied Biosystems). PCR conditions were 50°C for 2 min, 95°C for 10 min, and 40 cycles of 95°C for 15 s and 60°C for 1 min in an ABI Prism 7000 sequence detection system (Applied Biosystems). The relative levels of transcription in comparison with the internal control were analyzed according to the method of Hagihara et al. (53).

Statistical analysis. Statistica (ver. 10.0; StatSoft, OK, USA) was used to explore the differences between the mean values by applying Student's two-sample *t* test. A *P* value of <0.05 was considered significant.

Accession number(s). Newly determined sequence data have been deposited in NCBI/DDBJ under accession numbers LC427969, LC427970, LC427971, and LC427972.

SUPPLEMENTAL MATERIAL

Supplemental material for this article may be found at https://doi.org/10.1128/AEM.01977-18.

SUPPLEMENTAL FILE 1, PDF file, 1.4 MB.

ACKNOWLEDGMENTS

We appreciate the technical support of the environmental surveillance team of icddr,b. The thoughtful suggestions received from Prodyot Kumar Basu Neogi, formerly a scientist of icddr,b, are gratefully remembered.

This research was supported by the Osaka Prefecture University under the Monbukagakusho:MEXT scholarship and JASSO fellowship programs. icddr,b is thankful to the governments of Bangladesh, Canada, Sweden, and the United Kingdom for providing core/unrestricted support.

S.B.N. and N.C. designed and performed laboratory experiments and participated in data analysis. S.Y. and G.B.N. coordinated the experiments and analyzed the data. Z.H.M. and M.S.I. performed field studies. S.P.A., M.A., K.O., and A.H. helped design the study and participated in laboratory experiments. S.B.N., N.C., and S.Y. wrote the draft of the manuscript. All of us read and approved the final manuscript.

We declare that we have no conflict of interest.

REFERENCES

1. Safa A, Nair GB, Kong RY. 2010. Evolution of new variants of *Vibrio cholerae* O1. Trends Microbiol 18:46–54. https://doi.org/10.1016/j.tim.2009.10.003.
2. Rashed SM, Mannan SB, Johura FT, Islam MT, Sadique A, Watanabe H, Sack RB, Huq A, Colwell RR, Cravioto A, Alam M. 2012. Genetic characteristics of drug-resistant *Vibrio cholerae* O1 causing endemic cholera in Dhaka, 2006–2011. J Med Microbiol 61:1736–1745. https://doi.org/10.1099/jmm.0.049635-0.
3. Saidi SM, Chowdhury N, Awasthi SP, Asakura M, Hinenoya A, Iijima Y, Yamasaki S. 2014. Prevalence of *Vibrio cholerae* O1 El Tor variant in a cholera-endemic zone of Kenya. J Med Microbiol 63:415–420. https://doi.org/10.1099/jmm.0.068999-0.
4. Adewale AK, Pazhani GP, Abiodun IB, Afolabi O, Kolawole OD, Mukhopadhyay AK, Ramamurthy T. 2016. Unique clones of *Vibrio cholerae* O1 El Tor with Haitian type *ctxB* allele implicated in the recent cholera epidemics from Nigeria, Africa. PLoS One 11:e0159794. https://doi.org/10.1371/journal.pone.0159794.
5. Faruque SM, Rahman MM, Asadulghani NKMI, Mekalanos JJ. 1999. Lysogenic conversion of environmental *Vibrio mimicus* strains by CTXPhi. Infect Immun 67:5723–5729.
6. Boyd EF, Moyer KE, Shi L, Waldor MK. 2000. Infectious CTXΦ and the vibrio pathogenicity island prophage in *Vibrio mimicus*: evidence for recent horizontal transfer between *V. mimicus* and *V. cholerae*. Infect Immun 68:1507–1513. https://doi.org/10.1128/IAI.68.3.1507-1513.2000.
7. Bi K, Miyoshi SI, Tomochika KI, Shinoda S. 2001. Detection of virulence associated genes in clinical strains of *Vibrio mimicus*. Microbiol Immunol 45:613–616. https://doi.org/10.1111/j.1348-0421.2001.tb01292.x.
8. Islam MS, Rahman MZ, Khan SI, Mahmud ZH, Ramamurthy T, Nair GB, Sack RB, Sack DA. 2005. Organization of the CTX prophage in environmental isolates of *Vibrio mimicus*. Microbiol Immunol 49:779–784. https://doi.org/10.1111/j.1348-0421.2005.tb03668.x.
9. Wang D, Wang H, Zhou Y, Zhang Q, Zhang F, Du P, Wang S, Chen C, Kan B. 2011. Genome sequencing reveals unique mutations in characteristic metabolic pathways and the transfer of virulence genes between *Vibrio mimicus* and *Vibrio cholerae*. PLoS One 6:e21299. https://doi.org/10.1371/journal.pone.0021299.
10. Boyd EF, Heilpern AJ, Waldor MK. 2000. Molecular analysis of a putative CTXΦ precursor and evidence for independent acquisition of distinct CTXΦs by toxigenic *Vibrio cholerae*. J Bacteriol 182:5530–5538. https://doi.org/10.1128/JB.182.19.5530-5538.2000.
11. Dziejman M, Balon E, Boyd D, Fraser CM, Heidelberg JF, Mekalanos JJ. 2002. Comparative genomic analysis of *Vibrio cholerae*: genes that correlate with cholera endemic and pandemic disease. Proc Natl Acad Sci U S A 99:1556–1561. https://doi.org/10.1073/pnas.042667999.
12. Chatterjee S, Ghosh K, Raychoudhuri A, Chowdhury G, Bhattacharya MK, Mukhopadhyay AK, Ramamurthy T, Bhattacharya SK, Klose KE, Nandy RK. 2009. Incidence, virulence factors, and clonality among clinical strains of non-O1, non-O139 *Vibrio cholerae* isolates from hospitalized diarrheal patients in Kolkata, India. J Clin Microbiol 47:1087–1095. https://doi.org/10.1128/JCM.02026-08.
13. Awasthi SP, Asakura M, Chowdhury N, Neogi SB, Hinenoya A, Golbar HM,

Yamate J, Arakawa E, Tada T, Ramamurthy T, Yamasaki S. 2013. Novel cholix toxin variants, ADP-ribosylating toxins in *Vibrio cholerae* non-O1/non-O139 strains, and their pathogenicity. Infect Immun 81:531–541. https://doi.org/10.1128/IAI.00982-12.
14. Faruque SM, Mekalanos JJ. 2003. Pathogenicity islands and phages in *Vibrio cholerae* evolution. Trends Microbiol 11:505–510. https://doi.org/10.1016/j.tim.2003.09.003.
15. Waldor MK, Rubin EJ, Pearson GD, Kimsey H, Mekalanos JJ. 1997. Regulation, replication, and integration functions of the *Vibrio cholerae* CTXΦ are encoded by region RS*2*. Mol Microbiol 24:917–926. https://doi.org/10.1046/j.1365-2958.1997.3911758.x.
16. Moyer KE, Kimsey HH, Waldor MK. 2001. Evidence for a rolling-circle mechanism of phage DNA synthesis from both replicative and integrated forms of CTXΦ. Mol Microbiol 41:311–323. https://doi.org/10.1046/j.1365-2958.2001.02517.x.
17. Faruque SM, Asadulghani KM, Nandi RK, Ghosh AN, Nair GB, Mekalanos JJ, Sack DA. 2002. RS1 element of *Vibrio cholerae* can propagate horizontally as a filamentous phage exploiting the morphogenesis genes of CTXΦ. Infect Immun 70:163–170. https://doi.org/10.1128/IAI.70.1.163-170.2002.
18. Davis BM, Kimsey HH, Kane AV, Waldor MK. 2002. A satellite phage-encoded antirepressor induces repressor aggregation and cholera toxin gene transfer. EMBO J 21:4240–4249. https://doi.org/10.1093/emboj/cdf427.
19. Nandi S, Maiti D, Saha A, Bhadra RK. 2003. Genesis of variants of *Vibrio cholerae* O1 biotype El Tor: role of the CTXΦ array and its position in the genome. Microbiology 149:89–97. https://doi.org/10.1099/mic.0.25599-0.
20. Bhattacharya T, Chatterjee S, Maiti D, Bhadra RK, Takeda Y, Nair GB, Nandy RK. 2006. Molecular analysis of the *rstR* and *orfU* genes of the CTX prophages integrated in the small chromosomes of environmental *Vibrio cholerae* non-O1, non-O139 strains. Environ Microbiol 8:526–534. https://doi.org/10.1111/j.1462-2920.2005.00932.x.
21. Faruque SM, Tam VC, Chowdhury N, Diraphat P, Dziejman M, Heidelberg JF, Clemens JD, Mekalanos JJ, Nair GB. 2007. Genomic analysis of the Mozambique strain of *Vibrio cholerae* O1 reveals the origin of El Tor strains carrying classical CTX prophage. Proc Natl Acad Sci U S A 104:5151–5156. https://doi.org/10.1073/pnas.0700365104.
22. Mantri CK, Mohapatra SS, Colwell RR, Singh DV. 2010. Sequence analysis of *Vibrio cholerae orfU* and *zot* from pre-CTXΦ and CTXΦ reveals multiple origin of pre-CTXΦ and CTXΦ. Environ Microbiol Rep 2:67–75. https://doi.org/10.1111/j.1758-2229.2009.00085.x.
23. Waldor MK, Mekalanos JJ. 1996. Lysogenic conversion by a filamentous phage encoding cholera toxin. Science 272:1910–1914. https://doi.org/10.1126/science.272.5270.1910.
24. Skorupski K, Taylor RK. 1997. Control of the ToxR virulence regulon in *Vibrio cholerae* by environmental stimuli. Mol Microbiol 25:1003–1009. https://doi.org/10.1046/j.1365-2958.1997.5481909.x.
25. Mukhopadhyay AK, Chakraborty S, Takeda Y, Nair GB, Berg DE. 2001. Characterization of VPI pathogenicity island and CTXΦ prophage in environmental strains of *Vibrio cholerae*. J Bacteriol 183:4737–4746. https://doi.org/10.1128/JB.183.16.4737-4746.2001.
26. Tenover FC, Arbeit RD, Goering RV, Mickelsen PA, Murray BE, Persing DH, Swaminathan B. 1995. Interpreting chromosomal DNA restriction patterns produced by pulsed-field gel electrophoresis: criteria for bacterial strain typing. J Clin Microbiol 33:2233–2239.
27. Heilpern AJ, Waldor MK. 2003. pIIICTX, a predicted CTXΦ minor coat protein, can expand the host range of coliphage fd to include *Vibrio cholerae*. J Bacteriol 185:1037–1044. https://doi.org/10.1128/JB.185.3.1037-1044.2003.
28. Ford CG, Kolappan S, Phan HT, Waldor MK, Winther-Larsen HC, Craig L. 2012. Crystal structures of a CTX pIII domain unbound and in complex with a *Vibrio cholerae* Tol A domain reveal novel interaction interfaces. J Biol Chem 287:36258–36272. https://doi.org/10.1074/jbc.M112.403386.
29. Wang H, Pang B, Xiong L, Wang D, Wang X, Zhang L, Kan B. 2015. The hybrid pre-CTXΦ-RS1 prophage genome and its regulatory function in environmental *Vibrio cholerae* O1 strains. Appl Environ Microbiol 81:7171–7177. https://doi.org/10.1128/AEM.01742-15.
30. Halder K, Das B, Nair GB, Bhadra RK. 2010. Molecular evidence favouring step-wise evolution of Mozambique *Vibrio cholerae* O1 El Tor hybrid strain. Microbiology 156:99–107. https://doi.org/10.1099/mic.0.032458-0.
31. Kamruzzaman M, Robins WP, Bari SM, Nahar S, Mekalanos JJ, Faruque SM. 2014. RS1 satellite phage promotes diversity of toxigenic *Vibrio cholerae* by driving CTX prophage loss and elimination of lysogenic immunity. Infect Immun 82:3636–3643. https://doi.org/10.1128/IAI.01699-14.
32. Ghosh-Banerjee J, Senoh M, Takahashi T, Hamabata T, Barman S, Koley H, Mukhopadhyay AK, Ramamurthy T, Chatterjee S, Asakura M, Yamasaki S, Nair GB, Takeda Y. 2010. Cholera toxin production by the El Tor variant of *Vibrio cholerae* O1 compared to prototype El Tor and classical biotypes. J Clin Microbiol 48:4283–4286. https://doi.org/10.1128/JCM.00799-10.
33. Tikoo A, Singh DV, Sanyal SC. 1994. Influence of animal passage on haemolysin and enterotoxin production in *Vibrio cholerae* O1 biotype El Tor strains. J Med Microbiol 40:246–251. https://doi.org/10.1099/00222615-40-4-246.
34. O'Shea YA, Boyd EF. 2002. Mobilization of the *Vibrio* pathogenicity island between *Vibrio cholerae* isolates mediated by CP-T1 generalized transduction. FEMS Microbiol Lett 214:153–157. https://doi.org/10.1111/j.1574-6968.2002.tb11339.x.
35. Sarkar A, Nandy RK, Nair GB, Ghose AC. 2002. *Vibrio* pathogenicity island and cholera toxin genetic element-associated virulence genes and their expression in non-O1 non-O139 strains of *Vibrio cholerae*. Infect Immun 70:4735–4742. https://doi.org/10.1128/IAI.70.8.4735-4742.2002.
36. Kumar P, Thulaseedharan A, Chowdhury G, Ramamurthy T, Thomas S. 2011. Characterization of novel alleles of toxin co-regulated pilus A gene (*tcpA*) from environmental isolates of *Vibrio cholerae*. Curr Microbiol 62:758–763. https://doi.org/10.1007/s00284-010-9774-3.
37. Li F, Du P, Li B, Ke C, Chen A, Chen J, Zhou H, Li J, Morris JG, Jr, Kan B, Wang D. 2014. Distribution of virulence-associated genes and genetic relationships in non-O1/O139 *Vibrio cholerae* aquatic isolates from China. Appl Environ Microbiol 80:4987–4992. https://doi.org/10.1128/AEM.01021-14.
38. Kirn TJ, Lafferty MJ, Sandoe CM, Taylor RK. 2000. Delineation of pilin domains required for bacterial association into microcolonies and intestinal colonization by *Vibrio cholerae*. Mol Microbiol 35:896–910. https://doi.org/10.1046/j.1365-2958.2000.01764.x.
39. Reguera G, Kolter R. 2005. Virulence and the environment: a novel role for *Vibrio cholerae* toxin-coregulated pili in biofilm formation on chitin. J Bacteriol 187:3551–3555. https://doi.org/10.1128/JB.187.10.3551-3555.2005.
40. Boyd EF, Waldor MK. 2002. Evolutionary and functional analyses of variants of the toxin-coregulated pilus protein TcpA from toxigenic *Vibrio cholerae* non-O1/non-O139 serogroup isolates. Microbiology 148:1655–1666. https://doi.org/10.1099/00221287-148-6-1655.
41. Cervin J, Wands AM, Casselbrant A, Wu H, Krishnamurthy S, Cvjetkovic A, Estelius J, Dedic B, Sethi A, Wallom K-L, Riise R, Bäckström M, Wallenius V, Platt FM, Lebens M, Teneberg S, Fändriks L, Kohler JJ, Yrlid U. 2018. GM1 ganglioside-independent intoxication by cholera toxin. PLoS Pathog 14:e1006862. https://doi.org/10.1371/journal.ppat.1006862.
42. Nye MB, Pfau JD, Skorupski K, Taylor RK. 2000. *Vibrio cholerae* H-NS silences virulence gene expression at multiple steps in the ToxR regulatory cascade. J Bacteriol 182:4295–4303. https://doi.org/10.1128/JB.182.15.4295-4303.2000.
43. O'Shea YA, Reen FJ, Quirke AM, Boyd EF. 2004. Evolutionary genetic analysis of the emergence of epidemic *Vibrio cholerae* isolates on the basis of comparative nucleotide sequence analysis and multilocus virulence gene profiles. J Clin Microbiol 42:4657–4671. https://doi.org/10.1128/JCM.42.10.4657-4671.2004.
44. Hasan NA, Grim CJ, Haley BJ, Chun J, Alam M, Taviani E, Hoq M, Munk AC, Saunders E, Brettin TS, Bruce DC, Challacombe JF, Detter JC, Han CS, Xie G, Nair GB, Huq A, Colwell RR. 2010. Comparative genomics of clinical and environmental *Vibrio mimicus*. Proc Natl Acad Sci U S A 107:21134–21139. https://doi.org/10.1073/pnas.1013825107.
45. Davis BR, Fanning GR, Madden JM, Steigerwalt AG, Bradford HB, Smith HL, Brenner DJ. 1981. Characterization of biochemically atypical *Vibrio cholerae* strains and designation of a new pathogenic species, *Vibrio mimicus*. J Clin Microbiol 14:631–639.
46. Yamasaki S, Garg S, Nair GB, Takeda Y. 1999. Distribution of *Vibrio cholerae* O1 antigen biosynthesis genes among O139 and other non-O1 serogroups of *Vibrio cholerae*. FEMS Microbiol Lett 179:115–121. https://doi.org/10.1111/j.1574-6968.1999.tb08716.x.
47. Morita M, Ohnishi M, Arakawa E, Bhuiyan NA, Nusrin S, Alam M, Siddique AK, Qadri F, Izumiya H, Nair GB, Watanabe H. 2008. Development and validation of a mismatch amplification mutation PCR assay to monitor the dissemination of an emerging variant of *Vibrio cholerae* O1 biotype El Tor. Microbiol Immunol 52:314–317. https://doi.org/10.1111/j.1348-0421.2008.00041.x.
48. Iwanaga M, Yamamoto K, Higa N, Ichinose Y, Nakasone N, Tanabe M.

1986. Culture conditions for stimulating cholera toxin production by *Vibrio cholerae* O1 El Tor. Microbiol Immunol 30:1075–1083. https://doi.org/10.1111/j.1348-0421.1986.tb03037.x.
49. Chatterjee S, Asakura M, Chowdhury N, Neogi SB, Sugimoto N, Haldar S, Awasthi SP, Hinenoya A, Aoki S, Yamasaki S. 2010. Capsaicin, a potential inhibitor of cholera toxin production in *Vibrio cholerae*. FEMS Microbiol Lett 306:54–60. https://doi.org/10.1111/j.1574-6968.2010.01931.x.
50. Uesaka Y, Otsuka Y, Lin Z, Yamasaki S, Yamaoka J, Kurazono H, Takeda Y. 1994. Simple method of purification of *Escherichia coli* heat-labile enterotoxin and cholera toxin using immobilized galactose. Microb Pathog 16:71–76. https://doi.org/10.1006/mpat.1994.1007.
51. Oku Y, Uesaka Y, Hirayama T, Takeda Y. 1988. Development of a highly sensitive bead-ELISA to detect bacterial protein toxins. Microbiol Immunol 32:807–816. https://doi.org/10.1111/j.1348-0421.1988.tb01442.x.
52. Dean AG, Ching TC, Williams RG, Harden LB. 1972. Test for *Escherichia coli* enterotoxin in infant mice: application in a study of diarrhea in children in Honolulu. J Infect Dis 125:407–411. https://doi.org/10.1093/infdis/125.4.407.
53. Hagihara K, Nishikawa T, Isobe T, Song J, Sugamata Y, Yoshizaki K. 2004. IL-6 plays a critical role in the synergistic induction of human serum amyloid (SAA) gene when stimulated with proinflammatory cytokines as analyzed with an SAA isoform real-time quantitative RT-PCR assay system. Biochem Biophys Res Commun 314:363–369. https://doi.org/10.1016/j.bbrc.2003.12.096.
54. Marin MA, Vicente AC. 2012. Variants of *Vibrio cholerae* O1 El Tor from Zambia showed new genotypes of *ctxB*. Epidemiol Infect 140:1386–1387. https://doi.org/10.1017/S0950268811001944.
55. Thompson CC, Vicente AC, Souza RC, Vasconcelos AT, Vesth T, Alves N, Ussery DW, Iida T, Thompson FL. 2009. Genomic taxonomy of vibrios. BMC Evol Biol 9:258. https://doi.org/10.1186/1471-2148-9-258.
56. Zhang P, Zhou H, Kan B, Wang D. 2013. Novel *ctxB* variants of *Vibrio cholerae* O1 isolates, China. Infect Genet Evol 20:48–53. https://doi.org/10.1016/j.meegid.2013.08.004.
57. Hoshino K, Yamasaki S, Mukhopadhyay AK, Chakraborty S, Basu A, Bhattacharya SK, Nair GB, Shimada T, Takeda Y. 1998. Development and evaluation of a multiplex PCR assay for rapid detection of toxigenic *Vibrio cholerae* O1 and O139. FEMS Immunol Med Microbiol 20:201–207. https://doi.org/10.1111/j.1574-695X.1998.tb01128.x.
58. Olsvik Ø, Wahlberg J, Petterson B, Uhlen M, Popovic T, Wachsmuth IK, Fields PI. 1993. Use of automated sequencing of polymerase chain reaction-generated amplicons to identify three types of cholera toxin subunit B in *Vibrio cholerae* O1 strains. J Clin Microbiol 31:22–25.
59. Singh DV, Matte MH, Matte GR, Jiang S, Sabeena F, Shukla BN, Sanyal SC, Huq A, Colwell RR. 2001. Molecular analysis of *Vibrio cholerae* O1, O139, non-O1, and non-O139 strains: clonal relationships between clinical and environmental isolates. Appl Environ Microbiol 67:910–921. https://doi.org/10.1128/AEM.67.2.910-921.2001.